DISSERTATION

Novel Small Molecules for treatment of hepatocellular cancer

Neuartige kleine Moleküle zur Behandlung von Leberzellkrebs

zur Erlangung des akademischen Grades
Doctor medicinae (Dr. med.)

vorgelegt der Medizinischen Fakultät
Charité – Universitätsmedizin Berlin

von
Andi Ma

Erstbetreuer*in: Prof Dr. rer nat. Michael Höpfner

Datum der Promotion: 30. Juni 2024

Table of contents

List of tables

List of figures

List of abbreviations

HCC	Hepatocellular Carcinoma
TKIs	Tyrosine kinase inhibitors
RTKs	Receptor tyrosine kinases
IC50	Inhibitory Concentration needed to reduce activity to 50%
ROS	Reactive oxygen species
CAM	Chorioallantoic membrane assays
TNM	Tumor, lymph node, metastasis
BCLC	Barcelona Clinic Liver Cancer
LT	Liver transplantation
TACE	Transcatheter Arterial Chemoembolization
PD-1	Programmed cell death protein 1
VEGF	Vascular Endothelial Growth Factor
VEGFR	Vascular Endothelial Growth Factor Receptor
LDH	Lactate dehydrogenase
PI	Propidium iodide
PARP	Poly-(ADP-ribose)-polymerase

Abstract

Hepatocellular carcinomas (HCC) account for more than 80% of all primary liver cancers globally, making them the fourth leading cause of cancer-related death. Significant advancements have been achieved recently in surgical, interventional, and radiotherapy for early HCC. Advanced and metastatic HCC, however, continue to lack efficient medical therapy options, therefore, new systemic therapies are desperately needed. In this study, investigating the antineoplastic and antiangiogenic mode of action of two newly synthesized tyrosine kinase inhibitors (Thio-Iva and Thio-Dam) for cutting-edge medical HCC therapy using a coordinated set of *in vitro* and *in vivo* approaches.

Thio-Iva exhibited multikinase inhibitory action, with the most pronounced effects on VEGFR-2 (about 90%inhibition). Crystal violet and iCelligence were used to determine anti-proliferative effects, and Thio-Iva and Thio-Dam exhibited strong anti-proliferative effects in Huh-7 and SNU449 HCC cell lines at sub-micromolar or low micromolar IC50 values, were as follows: Thio-Iva (0.29 ± 0.18 µM and 0.53±0.32µM) and Thio-Dam (0.81±0.26µM and 1.64±0.51µM). Flow cytometry analysis demonstrated a significant cell cycle arrest in the G2/M phase, and western blot analysis revealed a similar reduction of Cyclin B1 in HCC cell lines treated with Thio-Iva and Thio-Dam. Fluorescence microscopy was used to measure the induction of reactive oxygen species (ROS) using the ROS-sensitive dye CellROX Orange. Apoptosis induction was measured with Caspase-3 activity ELISA, showing the apoptosis effects of Thio-Iva and Thio-Dam increased ROS-driven, mitochondria-associated apoptosis and caspase-3 activation. The antiangiogenic effects were investigated using tube formation experiments. The new compounds effectively inhibited the development of capillary tubes on human endothelial cells (EA. hy926) *in vitro*, indicating that they possess antiangiogenic properties. Finally, the antiangiogenic and antineoplastic effects of the new compounds *in vivo* were confirmed by performing chorioallantoic membrane assays (CAM assays). Notably, the novel compounds were more effective in reducing HCC tumour growth *in vivo* than the clinically relevant TK inhibitor Sorafenib.

Here, this study can demonstrate that two novel tyrosine kinase inhibitors, Thio-Iva and Thio-Dam, have significant anti-tumour and anti-angiogenic properties in HCC cell lines. It was shown that these new compounds can effectively attack the cellular processes and features of HCC cells that are acquired during the carcinogenic process. Based on the

findings of this study, Thio-Iva and Thio-Dam were effective in HCC cell lines, and further research is required to see whether these compounds may be employed as an alternative treatment.

Zusammenfassung

Hepatozelluläre Karzinome (HCC) machen weltweit mehr als 80 % aller primären Leberkrebserkrankungen aus und sind damit die vierthäufigste Ursache für krebsbedingte Todesfälle. Bei der chirurgischen, interventionellen und Strahlentherapie von HCC im Frühstadium wurden in letzter Zeit bedeutende Fortschritte erzielt. Für das fortgeschrittene und metastasierte HCC gibt es jedoch nach wie vor keine wirksamen medizinischen Behandlungsmöglichkeiten, weshalb neue systemische Therapien dringend erforderlich sind. In dieser Studie wird die antineoplastische und antiangiogene Wirkungsweise von zwei neu synthetisierten Tyrosinkinase-Inhibitoren (Thio-Iva und Thio-Dam) für eine innovative medizinische HCC-Therapie mit einer Reihe von koordinierten in vitro- und in vivo-Ansätzen untersucht.

Thio-Iva zeigte eine multikinasehemmende Wirkung, mit den ausgeprägtesten Effekten auf VEGFR-2 (etwa 90% Hemmung). Kristallviolett und iCelligence wurden verwendet, um die antiproliferativen Effekte zu bestimmen, und Thio-Iva und Thio-Dam zeigten starke antiproliferative Effekte in den Huh-7- und SNU449-HCC-Zelllinien bei submikromolaren oder niedrigen mikromolaren IC50-Werten, die wie folgt waren: Thio-Iva (0,29 ± 0,18 µM und 0,53±0,32µM) und Thio-Dam (0,81±0,26µM und 1,64±0,51µM). Die Durchflusszytometrie-Analyse ergab einen ausgeprägten Zellzyklus-Stillstand in der G2-M-Phase, und der Western Blot zeigte eine entsprechende Cyclin B1-Suppression in den HCC-Zelllinien nach der Behandlung mit Thio-Iva und Thio-Dam. Die Induktion reaktiver Sauerstoffspezies (ROS) wurde durch Fluoreszenzmikroskopie mit dem ROS-empfindlichen Farbstoff CellROX Orange bestimmt. Die Apoptoseinduktion wurde mit dem ELISA-Test für die Caspase-3-Aktivität gemessen, der die Apoptosewirkung von Thio-Iva und Thio-Dam durch ROS-getriebene, mitochondrien-assoziierte Apoptose und Caspase-3-Aktivierung zeigte. Die antiangiogenen Wirkungen wurden in vitro in an immortalisierten humanen Endothelzellen (Ea.Hy926) - untersucht. Hierbei wurde festgestellt, dass die neuen Verbindungen bei der Hemmung der Bildung kapillarähnlicher Strukturen wirksam sind. Schließlich wurden die antiangiogenen und antineoplastischen Wirkungen der neuen Verbindungen in vivo durch die Durchführung

von Chorioallantoismembran-Assays (CAM-Assays) bestätigt. Bemerkenswert ist, dass die neuen Verbindungen das Wachstum von HCC-Tumoren in vivo wirksamer reduzieren als der bereits zugelassene und klinisch relevante TK-Inhibitor Sorafenib.

Hier können wir zeigen, dass zwei neue Tyrosinkinase-Inhibitoren, Thio-Iva und Thio-Dam, signifikante Anti-Tumor- und Anti-Angiogenese-Eigenschaften in HCC-Zellen haben. Es konnte gezeigt werden, dass diese neuen Verbindungen die zellulären Prozesse und Merkmale von HCC-Zellen, die während des karzinogenen Prozesses erworben werden und als entscheidende Kennzeichen von Krebs bekannt sind, wirksam angreifen können. Ausgehend von den Ergebnissen dieser Studie waren Thio-Iva und Thio-Dam bei HCC-Zelllinien wirksam, und es sind weitere Forschungen erforderlich, um festzustellen, ob diese Verbindungen als alternative Behandlung eingesetzt werden können.

1 Introduction

1.1 State of the art – research

1.1.1 Hepatocellular Carcinoma

Primary liver cancer is expected to be the sixth most often diagnosed cancer and the third most common cause of cancer mortality in 2020, having morbidity and mortality rates greater for men than women in most countries(1). HCC is the most prevalent type of primary liver cancer, affecting 75-85% of patients followed by intrahepatic cholangiocarcinoma (15–20 %) and other rare types (5 %). Chronic hepatitis B and C virus infection, aflatoxin-contaminated food, alcohol abuse, obesity, type 2 diabetes, and smoking are the main risk factors for HCC(2). Patients are stratified according to the expected outcomes of their treatment in several proposals, such as tumor, lymph node, metastasis (TNM); the Chinese University Prognostic Index; Japanese Integrated Staging(3). However, since 1999, the Barcelona Clinic Liver Cancer (BCLC) staging classification has been used worldwide, divided into four stages, Early-stage (A), Intermediate-stage (B), Advanced-stage (C), and End-stage (D)(4), providing the basis for clinical prognosis and treatment.

1.1.2 Therapy

Since the last official update on BCLC prognosis and treatment strategies released in 2018, the available treatments for liver cancer have improved significantly(5,6). Here, we described the treatment regimens recommended for each BCLC stage (Figure 1). The early stage of HCC (BCLC 0) is characterized by a solitary tumor measuring less than 2 cm in patients with normal liver function and no cancer-related symptoms, without vascular infiltration or extrahepatic spread(7). Clinical management of this stage varies depending on the potential liver transplantation (LT) route. If liver transplantation is not possible, ablation would be the first step, which is similar to resection in terms of survival outcomes(8,9). Early stage (BCLC-A) is characterized as a single nodule or up to three multifocal nodules (all less than 3 cm) without macrovascular invasion, extrahepatic dissemination, or disease-related symptoms (PS-0)(7). For patients at this stage, we perform resection, with the option of transplantation or resection as appropriate. The intermediate stage (BCLC-B) is characterized as multifocal HCC, which is HCC that exceeds BCLC-A criteria, has intact liver function, produces no cancer symptoms (PS 0),

and does not penetrate the circulation or spread to other organs(7). The 2022 version of BCLC-B divides patients into three groups based on tumor burden and liver function. Transplantation, Transcatheter arterial chemoembolization (TACE), or systemic therapy can be chosen for different subgroups of patients. BCLC-C is defined as advanced, including patients with extrahepatic spread or vascular invasion and who remain relatively healthy as indicated by PS ≤2 at staging, and patients with BCLC-C should be considered for systemic therapy(7,10). End-stage BCLCs (BCLC-D) consist of patients with major cancer-related symptoms and/or impaired liver function, where LT is not an option due to HCC burden or non-HCC-related factors, and where short-term survival is low(7). A coordinated approach to palliative care and symptomatic management is necessary for this setting. The management of HCC is a multidisciplinary clinical decision based on the patient's condition, and although it is currently managed primarily through BCLC staging, it still has limitations. In short, liver transplantation, resection, and ablation are the main options for early-stage patients.

Since the majority of patients are already in the intermediate or advanced stages at the time of diagnosis, surgery and local treatment are largely irrelevant and systemic therapy becomes the primary treatment(5). However, no relevant clinical studies in HCC have shown a significant benefit of conventional chemotherapy, and therefore, systemic therapy to date has been dominated by Tyrosine kinase inhibitors (TKIs). Since the landmark SHARP trial in 2008, it has been demonstrated that sorafenib first-line treatment significantly improves overall survival by nearly 3 months compared to placebo in patients with advanced HCC(11). Since approximately ten years ago, sorafenib has been the only option for the standard systemic treatment of HCC, but it is chronically ineffective in most patients because of the early emergence of resistance, making the overall efficacy of the drug far from satisfactory. Lenvatinib was demonstrated in the REFLECT trial to be comparable to sorafenib till 2018(12). Then, for sorafenib-refractory or intolerant patients, data from the RESORCE and CELESTIAL studies showed that second-line treatment with regorafenib and cabozantinib significantly improved OS and PFS(13–15). Meanwhile, many drugs, including erlotinib(16), brivanib(17), and sunitinib(18), failed to show at least non-inferiority of sorafenib as first-line therapy in phase III clinical trials.

HCC appears to be particularly amenable to immunotherapies since cirrhosis has an immunosuppressive environment that can be altered by Immune checkpoint inhibitors(19). A cellular state that triggers upregulation in this condition is produced when programmed cell death protein 1(PD-1) receptors are upregulated in the presence of this situation. The

phase III CheckMate 459 research, however, found no appreciable distinction between the two arms receiving nivolumab or sorafenib, two anti-PD-1 medicines(20). As a result, nivolumab is not indicated for use as a primary monotherapy treatment for advanced HCC. Immunotherapies for HCC have their limitations, which means that more research and development work needs to be done to find novel therapeutic options.

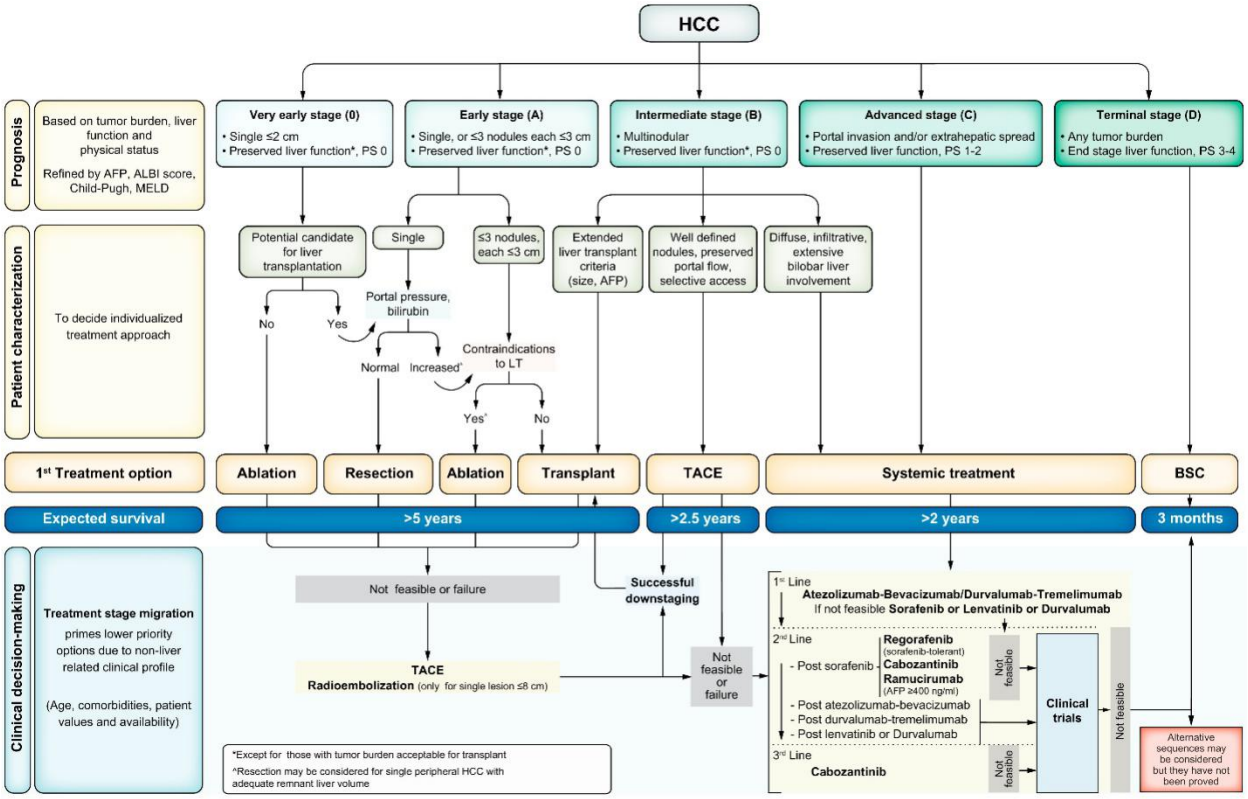

Figure 1: BCLC staging and treatment strategy in 2022. (Figure adapted from Reig M, Forner A, Rimola J, Ferrer-Fàbrega J, Burrel M, Garcia-Criado Á, Kelley RK, Galle PR, Mazzaferro V, Salem R, Sangro B, Singal AG, Vogel A, Fuster J, Ayuso C, Bruix J. J Hepatol. 2022)(7).

1.1.3 Angiogenesis role in HCC

Angiogenesis, which is primarily mediated by the vascular endothelial growth factors (VEGFs) and the receptor tyrosine kinases (RTKs) VEGFRs, plays a significant role in tumor growth and progression(21). HCC is a typical multi-vessel tumor and has been found to have significant angiogenesis and vascular abnormalities(22). VEGF is crucial for tumor angiogenesis and tumor development in HCC(23). Currently, all systemic therapies are molecularly targeted, and their main mechanism is anti-angiogenesis targeting VEGF and its receptors (Table 1). Although antiangiogenic therapies are well established and accepted in the treatment of HCC, antiangiogenic agents have exhibited substantial improvements over existing antiangiogenic agents. However, initial resistance

or drug resistance remains a major concern. A variety of different pathways may be involved in the angiogenic process. The development of anti-angiogenic therapies based on VEGFR antibodies and small molecule inhibitors holds great promise for preventing the growth and spread of aberrant tumor blood vessels, hence lowering tumor volume and hypoxia.

Table 1: Antiangiogenic therapies currently approved for HCC.

Name	Molecular targets	Clinical application
Sorafenib(11)	VEGFR-1–3, PDGFR-β, c-Kit, FLT-3, RET, Raf-1, B-Raf	first line therapy
Lenvatinib(12)	VEGFR1–VEGFR3, FGFR1–FGFR4, PDGFR, RET, and KIT	first/second-line therapy
Regorafenib(13)	VEGFR1–VEGFR3, RET, KIT, PDGFR, FGFR, B-RAF, RAF-1, p38, and TIE2	third-line therapy
Cabozantinib(14)	VEGFR1–VEGFR3, KIT, TIE2, MET, RET, and AXL	third/fourth-line therapy
Ramucirumab(24)	VEGFR2	third-line therapy
Bevacizumab(25)	VEGF	first-line therapy in combination with atezolizumab

1.1.4 Aims

New systemic medicines are urgently required since advanced stages of HCC currently have no viable medical therapy choices. Therefore, a set of novel small molecules 2-(thien-2-yl)-acrylonitrile derivatives with multi-kinase inhibitory activity (Figure 2) were developed and synthesized in collaboration with the Department of Organic Chemistry of

the University of Bayreuth, Germany (Prof. R. Schobert and Dr. B. Biersack). The aim of the project was to evaluate novel VEGF tyrosine kinase inhibitors for their antineoplastic and antiangiogenic properties in HCC.

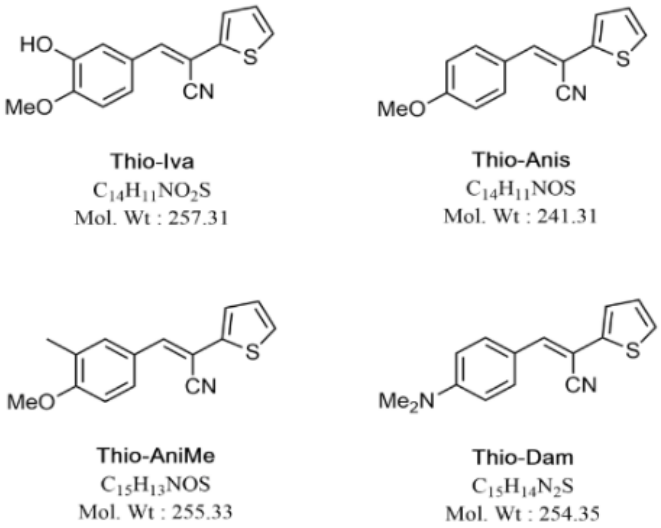

Figure 2: Chemical structures of E-2-(2-thienyl)-3-acrylonitrile RTK inhibitors were used in this study. (Figure adapted from Ma A, Biersack B, Goehringer N, Nitzsche B, Höpfner M. J Pers Med. 2022)(26).

2 Methods

Please refer to the "Methods" section of the publication for a comprehensive explanation of the research approach that was taken for the study. (Ma A, Biersack B, Goehringer N, Nitzsche B, Höpfner M. J Pers Med. 2022)(26). A brief overview is provided as follows.

2.1 Compounds

Stock solutions of Thio-Iva, Thio-Dam, Thio-Anis, and Thio-Anime were synthesized and provided by Dr. Biersack (Dept. of Organic Chemistry, University of Bayreuth, Germany)(27). Sorafenib was bought via Targetmol (T0093L, Boston, USA).

2.2 Biological Evaluation

2.2.1 Cell culture

Human hepatocellular carcinoma cell line Huh-7 (JCRB#0403) was cultured in 10% fetal bovine serum, 100 U/mL penicillin, and 100 mg/mL streptomycin-supplemented RPMI 1640 medium (Thermo Fisher Scientific, Inc.). In addition, the SNU-449 cells (ATCC#2234) were more add 1%HEPES, and 1% sodium pyruvate. Human umbilical vein EA. hy926 cells were cultured in DMEM. All cells were incubated at 37 °C, 5% CO_2, and 95% relative humidity.

2.2.2 Crystal violet staining

The light extinction of crystal violet, which increases linearly with cell population, was measured at 570 nm 30 using an ELISA reader(Dynex Technologies, Dunkeldorf, Germany).(27)

2.2.3 Real-time cell proliferation monitoring

As previously disclosed, cell real-time growth and survival were tracked using the iCELLigence System (ACEA Biosciences)(26).

2.2.4 Colony formation assay

Only cells comprising more than 50 cells were counted, as colonies were defined as aggregates of cells containing 50 or more cells(28). A kappa digital camera system

captured representative photographs (Kappa Optronics GmbH, Germany). Colony Area ImageJ plug-in was utilized to quantify stained colonies(28) (Vision 1.52a, National Institutes of Health, USA).

2.2.5 Determination of caspase-3

Cleaved caspase-3 cleaves AC-DEVD-AMC (EMD Millipore, Billerica, MA, USA), to produce fluorescent AC-DEVD, which was measured by microplate luminometer (Thermo Fisher Scientific, Waltham, MA, USA; filter sets: ex 360/40 nm, em 460/10 nm).(29)

2.2.6 Lactate dehydrogenase (LDH) assay

Cytotoxicity was tested by the LDH leakage to the cell surface, using an ELISA reader (Dynex Technologies, Dunkeldorf, Germany), at 490/630 nm.(26)

2.2.7 Scratch assay

The cells were cultured for 24 hours before being photographed using an EVOS M5000 microscope (Thermo Fischer Scientific, Waltham MA, USA). TScratch software (CSElab) was used to quantify cell migration, and migration results were normalized to control and set to 100%.(26)

2.2.8 Measurement of Reactive Oxygen Species (ROS)

After oxidation, membrane permeable dye CellROX® Orange (Thermo Fisher Scientific) emits a strong fluorescent signal. ZOETM Fluorescent Cell Imager evaluated ROS formation after 24h of compound incubation (Biorad, Munich Germany).

2.2.9 Flow cytometry cell cycle analysis

Flow cytometry was employed to examine the cell cycle by staining the DNA of treated HCC cells with propidium iodide (PI) (Invitrogen, Eugene, Oregon, USA). Using FACSCanto II, samples were examined (BD Biosciences). The FlowJo 10.4 program was utilized for data analysis (BD).(26)

2.2.10 Tube Formation

Cell culture used Matrigel (CorningTM 354234, MA, USA). EVOS M5000 microscope photos were taken (Thermo Fischer Scientific, Waltham MA, USA). The ImageJ

Angiogenesis Analyzer plugin was used to quantify tube development. Total segment length was reported.

2.2.11 Western blot

Cyclin B1 (H-443 Santa Cruz Biotechnology, 1:1000), poly-(ADP-ribose)-polymerase (PARP) and cleaved PARP (11835238 Roche, 1:1000), and β-actin (A5441 Sigma Aldrich, 1:2000) antibodies were employed. Incubation with anti-mouse (NA931VS Santa Cruz Biotechnology, 1:10000) or anti-rabbit (NA934VS Santa Cruz Biotechnology, 1:10000) peroxidase-coupled anti-IgG secondary antibodies. Clarity Max ECL Western Blotting substrate (Biorad, Munich, Germany) and Celvin-S developer identified and produced antibody binding (Biostep, software SnapAndGo).

2.2.12 Chicken chorioallantoic membrane assay (CAM)

Fertilized chicken eggs from Valo Biomedia GmbH, Germany, were incubated at 37.8°C and 66% relative humidity. Cutting the top shell opened the eggs on day 3.
A 5-mm silicone ring was connected to the CAM for 24 hours for anti-angiogenesis test. Day12: pipetting compounds. After 48h, a digital camera recorded CAM blood vessel condition (Distelkamp-Electronic, Kaiserslautern, Germany). Image Pro Plus 6.0 measured blood vessel length to quantify angiogenesis (Image-pro Plus, Media Cybernetics, Inc., USA).
Tumors were seeded on the CAM of fertilized eggs on day 8 of embryonic development and treated with the chemicals for 72 hours before being carefully removed and weighed for anti-neoplastic test.

2.2.13 Statistical analysis

GraphPad 8.00 (San Diego, California, USA) was utilized for statistical analysis. All tests were performed 3-5 times and reported as means +/- SD or SEM, unless otherwise stated. One-way analysis of variance determined statistical significance (ANOVA).

3 Results

3.1 HCC cell IC50 measurement of thiophene-based substances

The growth inhibition of four thiophene-based test compounds were tested on the Huh-7 and SNU-449 cell lines of HCC using crystal violet staining assay. For Huh-7, the IC50 values of four compounds, Thio-Iva, Thio-Dam, Thio-Anis, and Thio-AniMe, as well as the clinically authorized VEGFR inhibitor sorafenib, were as follows: 0.29 ± 0.18 μM, 0.81±0.26 μM, 1.20±0.42 μM, 1.85±0.21 μM and 2.50±0.14 μM after 48h of treatment (Table 2). For SNU-449, Thio-Iva and Thio-Dam demonstrated significant antiproliferative effects with IC50 values of 0.53±0.32 μM and 1.64±0.51 μM, both of which were significantly lower than sorafenib with IC50 >8 μM. Therefore, we selected Thio-Iva and Thio-Dam, the two compounds that worked best in all cell lines, for the following studies.

Table 2: Determination of IC50 values (μM) of test compounds for HCC cell lines after 48h incubation

Compounds	Huh-7	SNU-449
Thio-Iva	0.29±0.18	0.53±0.32
Thio-Dam	0.81±0.26	1.64±0.51
Thio-Anis	1.20±0.42	>8
Thio-AniMe	1.85±0.21	>8
Sorafenib	2.50±0.14	>8

3.2 Antiproliferative Activity in HCC Cells

We employed the iCELLigence system to non-invasively monitor cell growth in real-time to further assess the impact of the chemicals on HCC proliferation. Real-time resistance measurement data will be recorded and provided with a unitless quantity known as Cell Index (CI), which represents cell number and viability, the higher the cell index, the higher the cell viability. It can thus be seen that both Huh-7 and SNU-449 cells exhibit growth inhibition in the control group (Figure 3). Both cell lines that were treated with Thio-Iva (0.1- 1.0 μM) had dose-dependent CI values.

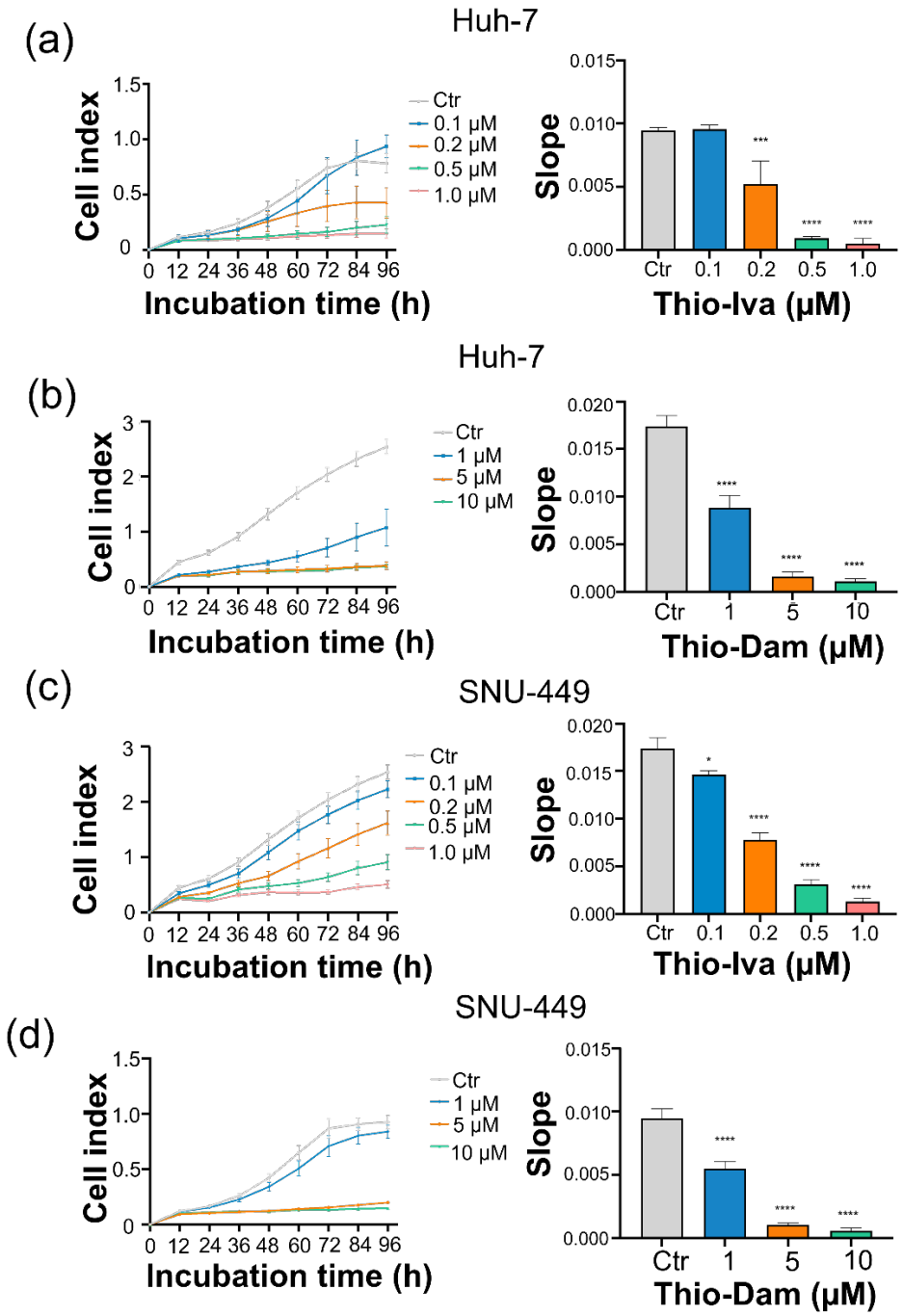

Figure 3: Real-time proliferation. iCELLigence system was used for Huh-7 (a, b) and SNU-449 (c, d) cells with different concentration of Thio-Iva and Thio-Dam on cell index and slope. Statistical significance *$P < 0.05$, ***$P < 0.001$ and ****$P<0.0001$ by ordinary one-way ANOVA as compared to untreated control (mean ± SEM of at least n=3). (Figure adapted from Ma A, Biersack B, Goehringer N, Nitzsche B, Höpfner M. J Pers Med. 2022)(26).

In line with the long-time proliferation analysis, we noted that plates seeded with Huh-7 and SNU-449 (Figure 4) cell lines contained a 50% reduction in the area of clones after

treatment with low concentration Thio-Iva, and the plates using Thio-Dam also suggested a good ability to inhibit clone formation, for incubating about 14 days.

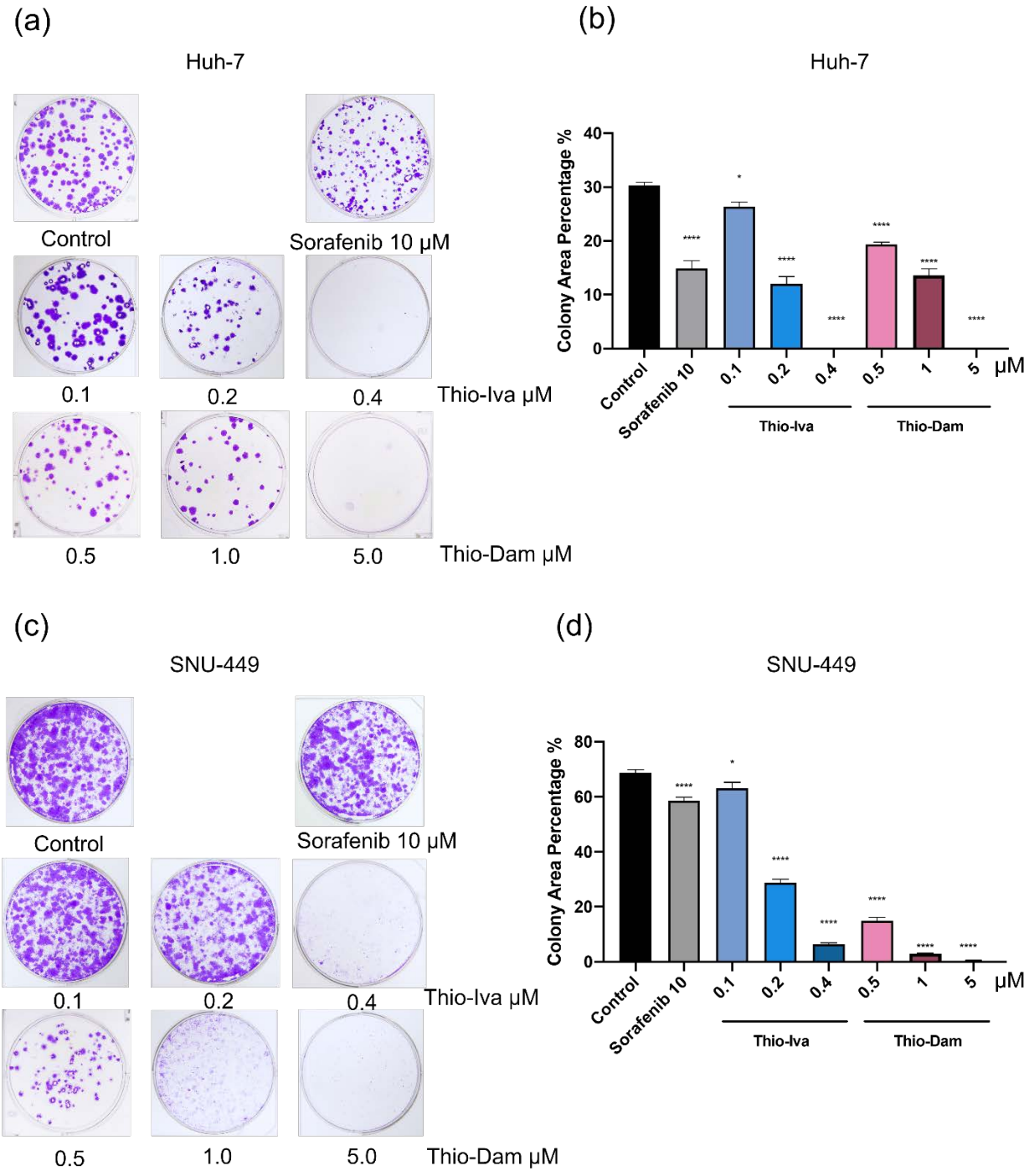

Figure 4: Clonogenic growth. Treatment with Thio-Iva, Thio-Dam, and Sorafenib of Huh-7 (a, b), SNU-449 (c, d) (Figure adapted from Ma A, Biersack B, Goehringer N, Nitzsche B, Höpfner M. J Pers Med. 2022)(26). *P < 0.05 and ****P<0.0001 by ordinary one-way ANOVA compared to control (non-treated) (mean ± SEM of at least n=3).

3.3 Unspecific cytotoxicity

The cytotoxicity of damaged cells was assessed by measuring the amount of LDH released into supernatants compared to LDH released from control cells. Huh-7 and SNU-449 cells were incubated with four compounds for 6 and 24 hours with compounds being tested at a low concentration of 1.0 µM and a high concentration of 10.0 µM. The results showed no apparent increase in LDH release, even at the highest concentration (Figure 5). Cells were incubated for 6 and 24 hours and the non-specific cytotoxicity only rose by about 5%. Thus, the induced cytotoxicity cannot explain the observed antiproliferative effect of these inhibitors.

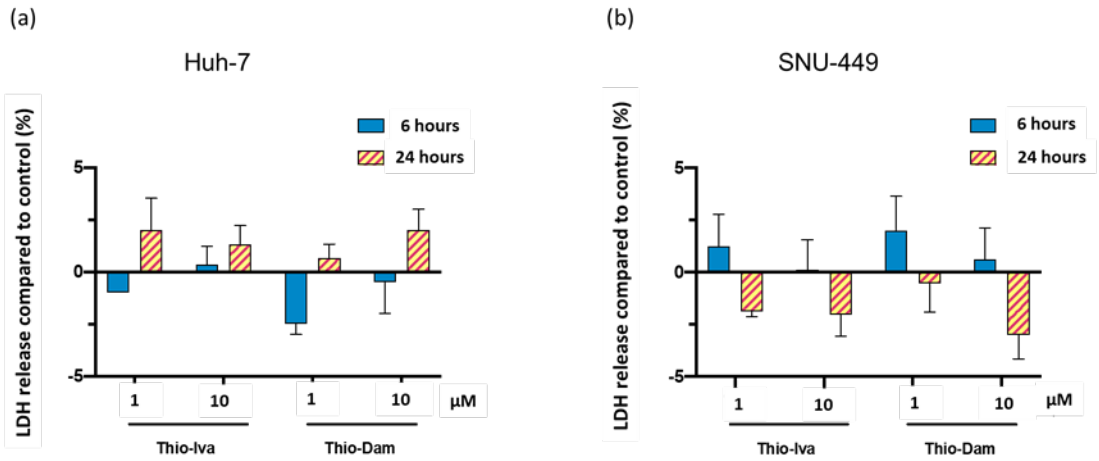

Figure 5: LDH release detection for all compounds. Cytotoxicity was evaluated by LDH release as a percentage of control LDH release. (a)Huh-7 (b) SNU-449. All compounds were incubated for 6 h and 24 h using two concentrations of 1.0 µM and 10.0 µM. (mean ± SEM of at least n=3). (Figure adapted from Ma A, Biersack B, Goehringer N, Nitzsche B, Höpfner M. J Pers Med. 2022)(26).

3.4 Apoptosis induction and regulation of Thio-Iva and Thio-Dam.

The apoptotic program has long been widely recognized as being closely associated with cancer. The Caspases family plays a crucial role in apoptosis execution, comprising the apoptosis promoter caspase-2,8,9,10 and the executors caspase- 3,6,7(30). Caspase-3 is an example of a common downstream effector component that is present in the majority of apoptotic pathways. It plays an essential part in the apoptotic process. When caspase-3 is activated it becomes cleaved caspase-3, so detecting cleaved caspase-3 is a common marker for apoptosis(31).

Our data show Thio-Iva and Thio-Dam significantly and dose-dependently increased cleaved caspase-3 in Huh-7 and SNU-449 cells, with a higher intensity than that induced by sorafenib (10 µM). Compared to untreated cells, Thio-Iva with 1.0 µM for Huh-7 cell line led to a 3-fold increase after 48 h, and for 10.0 µM with a 5.5-fold increase. For SNU-449 cell line 10.0 µM also increased 3-fold and 5.5 -fold more than after 48 h. And For Thio-Dam in Huh-7 cell line after 48h, the increase was 3.5-fold and 5-fold both in low and high concentration. But for SNU-449 cells not. In both Huh-7 and SNU-449 cells, our compounds induced a more pronounced cleaved caspase-3 than sorafenib (10 µM) (Figure 6a, b). Western blot investigations demonstrated that poly-(ADP-ribose)-polymerase (PARP) cleavage was increased in both cell lines when treated with Thio-Iva groups (Figure 6c), whereas the effect of Thio-Dam was less prominent in SNU-449 cells or even missing in Huh-7 cells.

ROS are responsible for cell damage and trigger mitochondria-driven apoptosis due to the increased formation of reactive oxygen species. The dye particular for ROS Huh-7 cells were stained with CellROX orange to identify Thio-Iva and Thio-Dam-induced ROS production in the cytoplasm. After 24 h of treatment, the cytoplasm of treated cells demonstrated a dose-dependent increase in ROS. (Figure 6d).

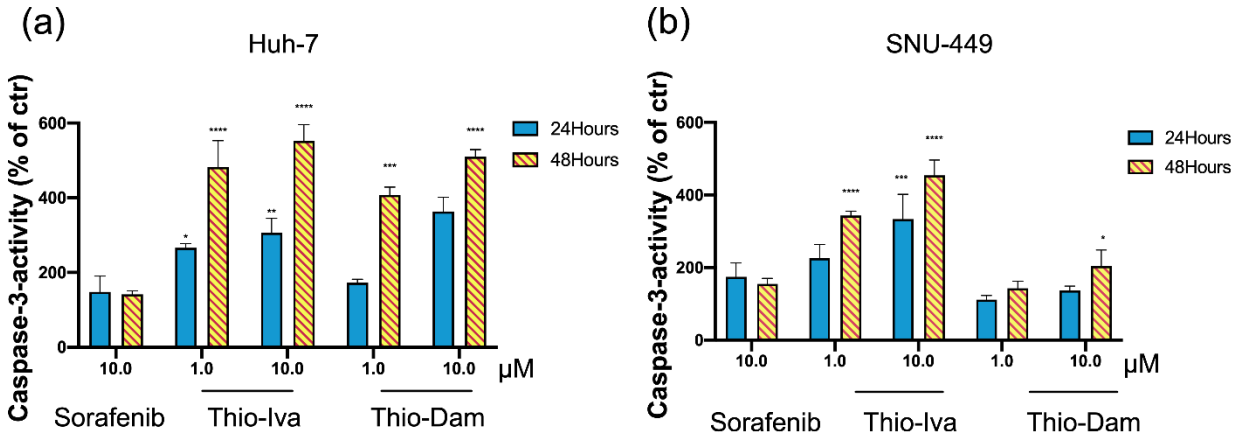

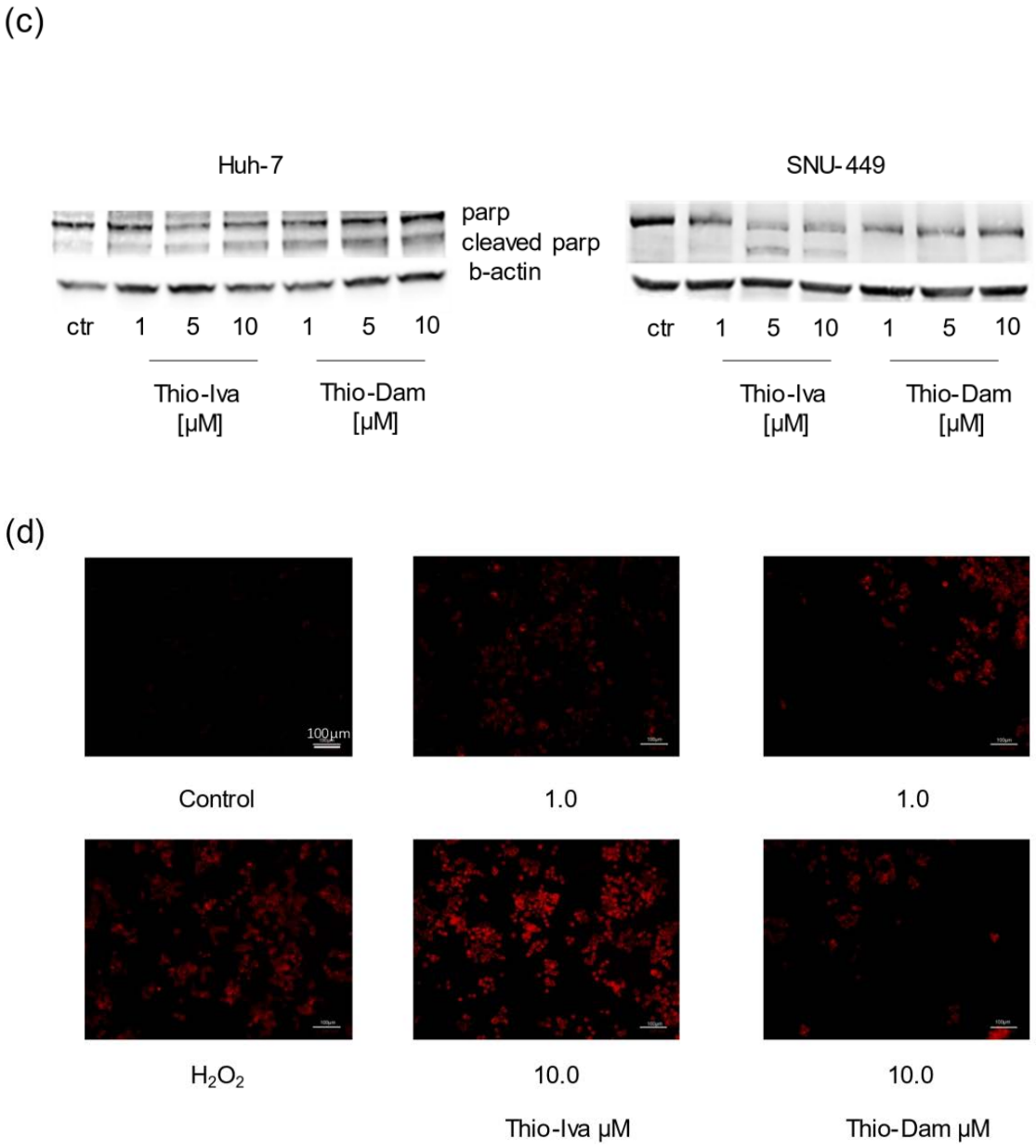

Figure 6: Induction of Apoptosis. (a,b) Induction of caspase-3 in Huh-7 and SNU-449 cells that is both dose- and time-dependent. *$P < 0.05$, **$P < 0.01$, ***$P < 0.001$ and ****$P<0.0001$ by ordinary one-way ANOVA compared to untreated controls. (mean ± SEM of at least n=3). (c) After 48 hours, representative Western blot result from n=3 independent studies demonstrating the effect of treatment on PARP and cleaved PARP expression in Huh-7 and SNU-449 cells. ß-actin was used as a loading control. (d) After 24 hours, detection of ROS induction by Thio-Iva and Thio-Dam in HCC cells. H_2O_2 served as a positive control. Scale bar, 100 µm. (Figure adapted from Ma A, Biersack B, Goehringer N, Nitzsche B, Höpfner M. J Pers Med. 2022)(26).

3.5 Cell-cycle regulation

The cell cycle regulation of Thio-Iva and Thio-Dam in HuH-7 and SNU449 cells was investigated using flow cytometry. Compared to sorafenib, HCC cells treated with Thio-Iva and Thio-Dam for 48 hours shown a dose-dependent G2-M phase block (Figure 7). Cyclin B1 is a checkpoint regulatory protein that is thought to regulate translocation to the nucleus and the onset of mitosis at the G2/M checkpoint(32). The degradation of cyclin B1 is required for cell detachment from mitosis. To further investigate the molecular mechanism of G2-M phase blocking, the expression of the cell cycle promoter Cyclin B1 was measured. After 48 hours of incubation, high quantities of Thio-Iva and Thio-Dam reduced cyclin B1 expression (Figure 7), supporting the flow cytometry results.

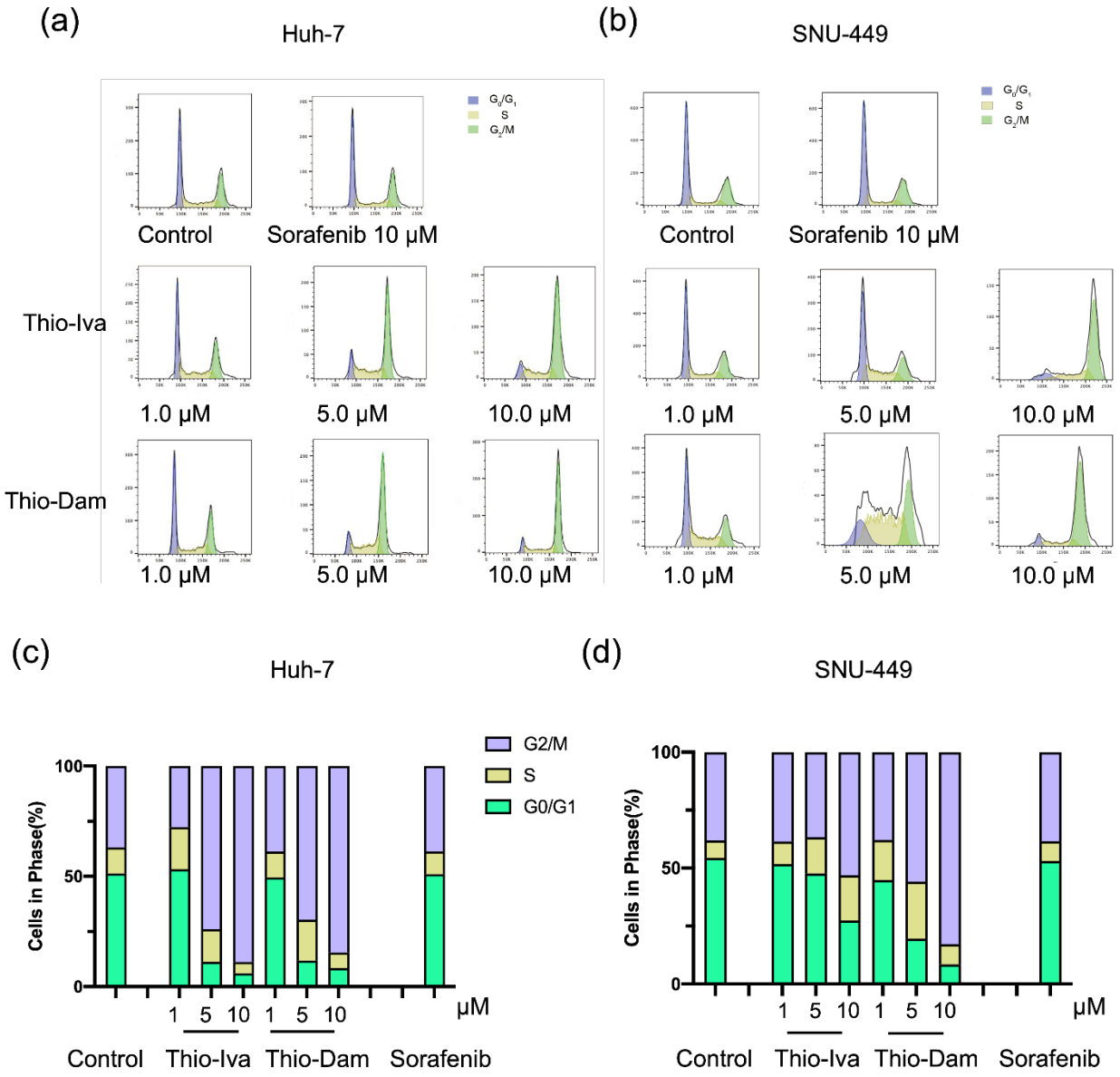

(e)

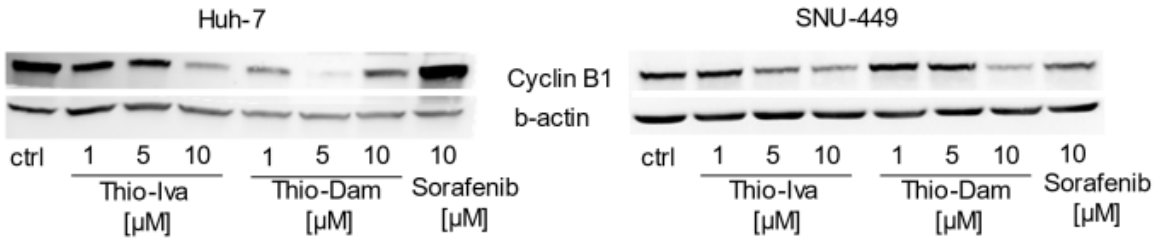

Figure 7: Influence on the cell cycle. Propidium iodide (PI) staining showed induced G2/M cell-cycle block, Huh-7(a), and SNU-449(b). The histogram displays the average results of quantifying the rate of all cell cycles, Huh-7(c) and SNU-449(d). (mean ± SEM of at least n=3). (e) Representative Western blots from n=3 separate studies demonstrating a change in Cyclin B1 expression caused by treatment in Huh-7 and SNU-449 cells after 48 hours. As a loading control, ß-actin was employed. (Figure adapted from Ma A, Biersack B, Goehringer N, Nitzsche B, Höpfner M. J Pers Med. 2022)(26).

3.6 Inhibition of cell migration

Thio-Iva and Thio-Dam were tested for HCC cell motility in scratch experiments (Figure 8). Huh-7 cells treated with Thio-Iva (1, 5, and 10 µM) showed a dose-dependent decrease in migration rate of 33.0%, 19.0%, and 10.0%. Thio-Dam (1, 5, and 10 µM) migrated at 28.0%, 21.3%, and 16.0%, like Thio-Iva (Figure 8a, c). Thio-Iva (1, 5, 10 µM) reduced SNU-449 cell migration from 49.3% to 18.3%, 4.6%, and 2.3%. Thio-Dam (1, 5, 10 µM) reduced SNU-449 migration rates by 8.7%, 2.0%, and 1.7%. (Figure 8b, d).

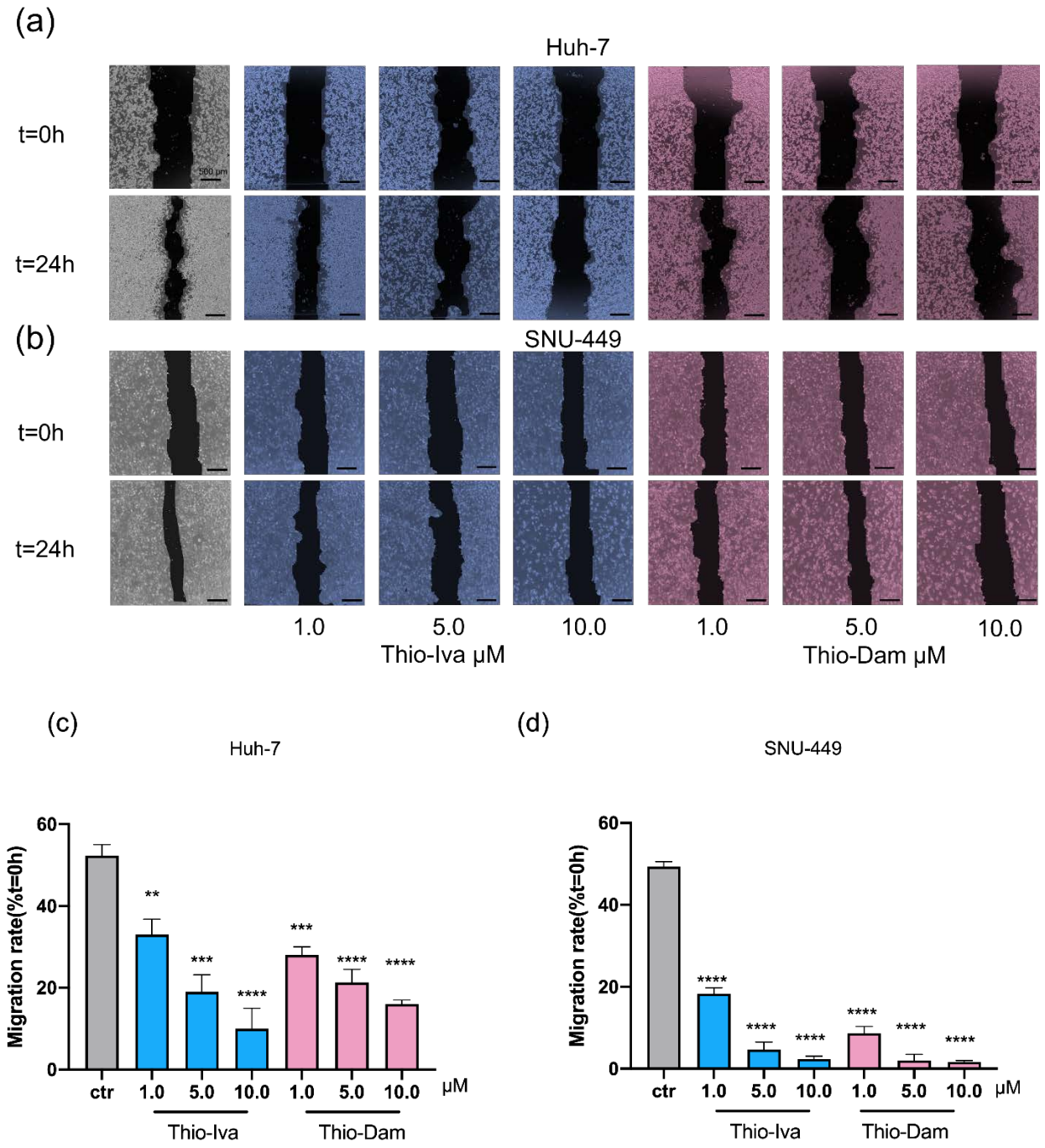

Figure 8: The influence of migration using scratch assays. Representative photos of the antimigratory effects of Thio-Iva and Thio-Dam on Huh-7(a) and SNU-449 (b) after 24 hours of incubation, as evidenced by the repressed closure of the open image region. (c) (d) The migration rate (in percent) after 0 and 24 hours of incubation. $^{**}P < 0.01$, $^{***}P < 0.001$ and $^{****}P<0.0001$ by ordinary one-way ANOVA compared to control(non-treated). (mean ± SEM of at least n=3). Scale bar, 500 µm. (Figure adapted from Ma A, Biersack B, Goehringer N, Nitzsche B, Höpfner M. J Pers Med. 2022)(26).

3.7 Antiangiogenic effects *in vitro* and *in vivo*

Angiogenesis, a hallmark of tumors, is a necessary process for tumor development. So, to evaluating the effect of Thio-Iva and Thio-Dam in angiogenesis. First, tube formation assays with human endothelial cells EA.hy 926 was performed *in vitro* (Figure 9). Thio-Iva treatment revealed substantial inhibition even at low doses (e.g., 0.2 µM) compared to the control, with a 51% reduction in fragment length and up to 92% inhibition for 1.0 µM. Even though the inhibition effect of Thio-Dam treatment was not very high, for the 1.0 µM treatment, the segment length of the tube was reduced by 69%.

Based on experimental results, a chicken CAM assay was employed to determine angiogenesis responses *in vivo*. We placed a silicone ring (1.5 mm) on the top of CAM, pipetting Thio-Iva, Thio-Dam, and Sorafenib solution into the ring, as a control outside the ring. Thio-Iva and Thio-Dam showed a strong reduction in angiogenesis, even severer than the known anti-angiogenic drug sorafenib. Compared to the control group, the vessels exhibited morphological abnormalities (Figure 9). Observations from the same vascular location indicate that Thio-Iva and Thio-Dam decreased angiogenesis *in vivo* with dose-dependent.

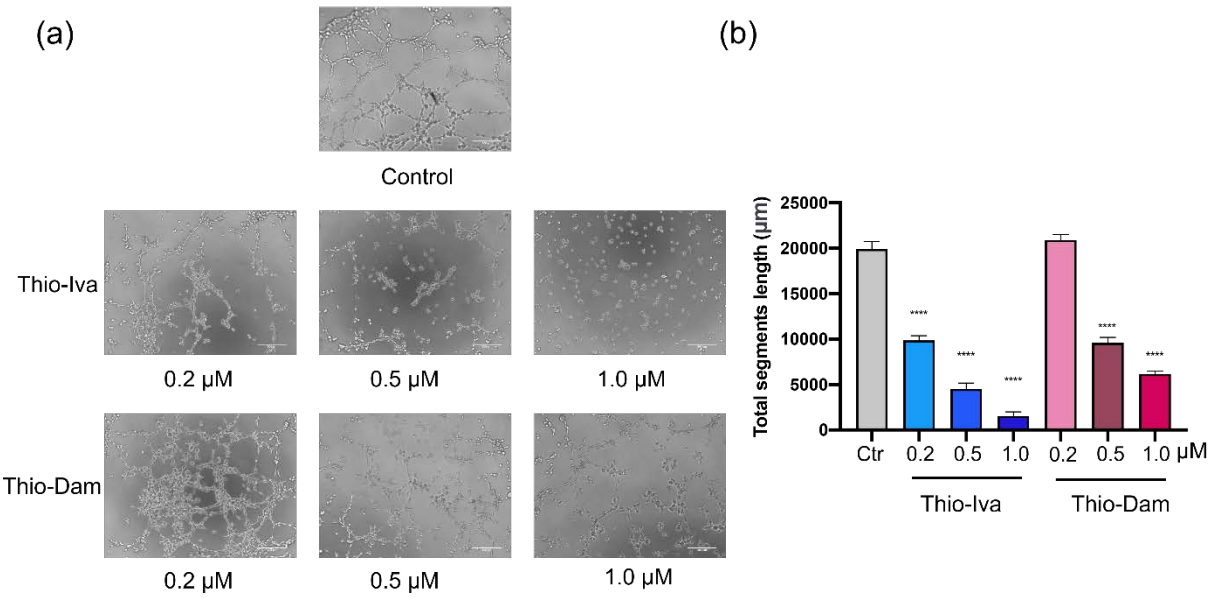

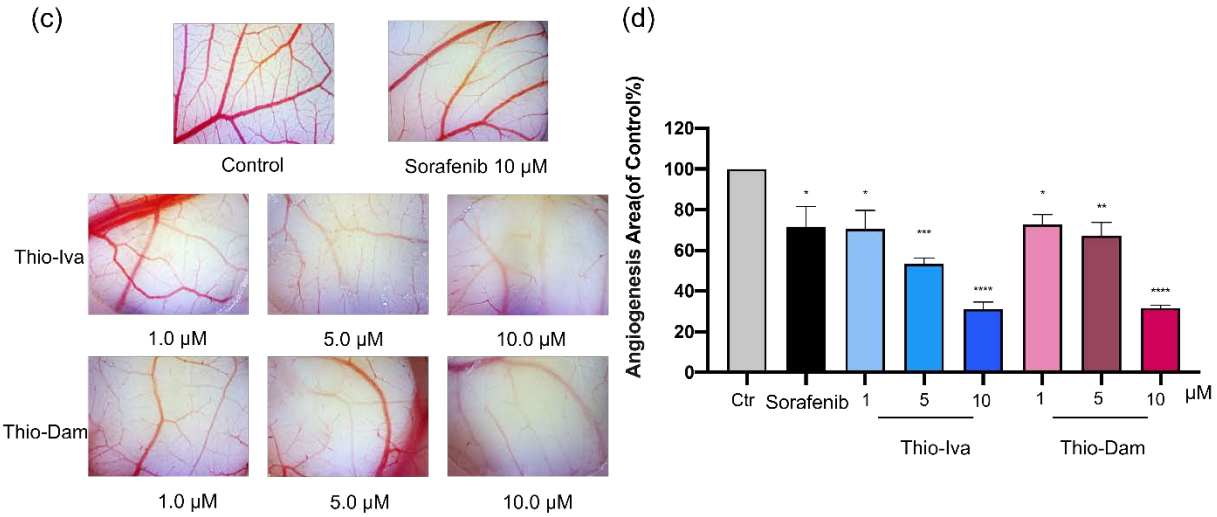

Figure 9: The effect of Angiogenesis *in vitro* and *in vivo*. (a) Representative images of tube formation assay, Scale bar, 500 µm. (b) Tube formation quantification by ImageJ software. c) Examples of CAM assays from a typical experiment demonstrating suppression of angiogenesis *in vivo*. The control material consists of untreated silica ring material. The interior of the silica ring was treated with Thio-Iva and Thio-Dam for 48 hours. (d) Blood vessel area quantification. (Compare to control in %). *P < 0.05, **P < 0.01, ***P < 0.001 and ****P<0.0001 by ordinary one-way ANOVA compared to control (no ntreated). (mean ± SEM of at least n=3). (Figure adapted from Ma A, Biersack B, Goehringer N, Nitzsche B, Höpfner M. J Pers Med. 2022)(26).

3.8 Antineoplastic effects *in vivo*

HuH-7 cell-derived microtumors were seeded onto CAM and treated for up to 72 hours with Thio-Iva (1.0-10.0 M) and Thio-Dam (1.0-10.0 M), showing higher inhibition of tumor growth in developing embryonic CAM compared to untreated control groups, and Thio-Iva and Thio-Dam 10.0 µM treatment groups reduced tumor weight by 62% and 71%, respectively, and resulted in a dose-dependent inhibition of tumor growth (Figure 10). Moreover, there was no significant difference in embryonic lethality between eggs treated with these compounds. Furthermore, sorafenib did not significantly inhibit Huh7 microtumor growth. In their respective LDH-release experiments, neither Thio-Iva nor Thio-Dam exhibited nonspecific harmful effects, as evidenced by the absence of increased embryonic lethality or signs of developmental delay in treated eggs.

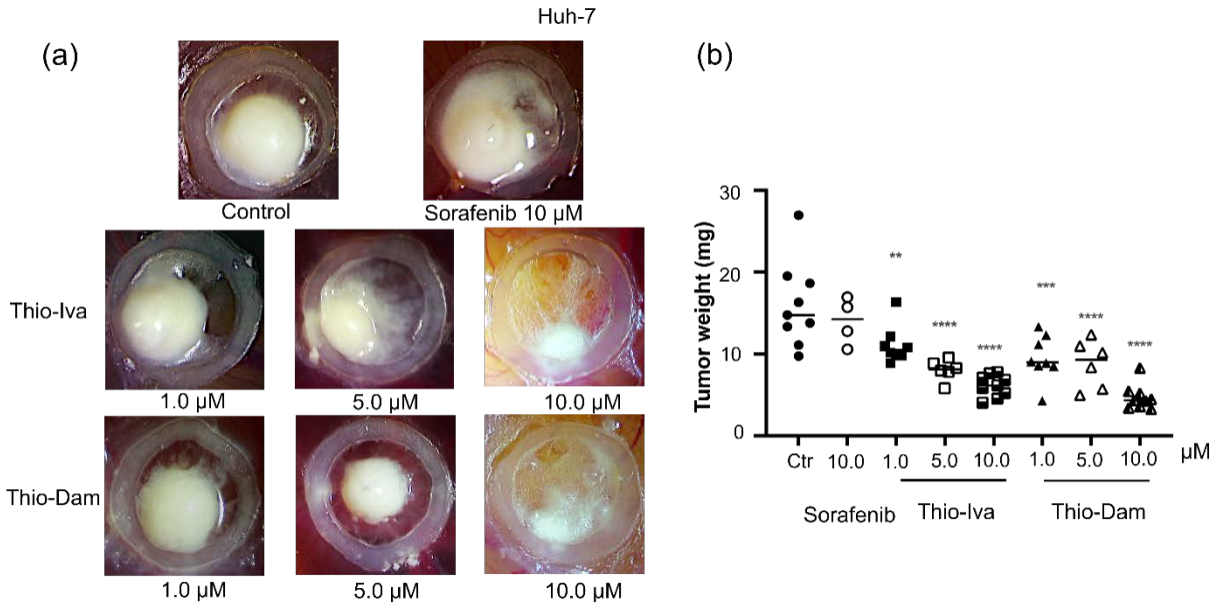

Figure 10: The effect of Anti-neoplastic *in vivo*. (a) Representative images of CAM assay, the microtumor was inoculated by mixing HuH-7 cells and matrigel and treated with Thio-Iva and Thio-Dam in different concentrations and Sorafenib for about 72h, untreated as control. (b) Calculate and analyze the weight of the tumor. (Figure adapted from Ma A, Biersack B, Goehringer N, Nitzsche B, Höpfner M. J Pers Med. 2022)(26). *P < 0.05, **P < 0.01, ***P < 0.001 and ****P<0.0001 by ordinary one-way ANOVA compared to control(nontreated). (mean ± SEM of at least n=3).

4 Discussion

4.1 Short summary of the effect.

For the possible therapy of HCC, four new thienyl-based tyrosine kinase inhibitors were created in this work. Compared to sorafenib and the other two inhibitors, Thio-Iva and Thio-Dam have demonstrated superior antiproliferative action in typical HCC cell lines in terms of cell viability, cell proliferation, and colony formation. Therefore, Thio-Iva and Thio-Dam were chosen to focus on rest of this study. Thio-Iva significantly induced apoptosis with an increased cleaved caspase-3, increased cleaved PARP expression and induction of ROS in HCC cell lines, while Thio-Dam showed a minder effect. Both Thio-Iva and Thio-Dam induced cell cycle block in the G2-M phase and induced the degradation of cyclin B1 with dose-dependent. Result showed that the migration of HCC cells was inhibited with the treatment of Thio-Iva and Thio-Dam. In addition, Thio-Iva and Thio-Dam showed strong inhibition of tube formation in vitro and strong reduction of angiogenesis of blood vessels *in vivo*. Further, Thio-Iva and Thio-Dam showed a strong inhibition of tumor growth *in vivo*. In addition, none of the substances induced cell cytotoxicity, as determined by LDH release, and there was no evidence of embryonic mortality or developmental retardation in the CAM experiment. Our results indicated that Thio-Iva and Thio-Dam have anti-proliferative, apoptosis-inducing, anti-migration, cell cycle arrest, antiangiogenic, and antitumor effects in HCC. And Thio-Iva had more extensive and stronger antiangiogenic and antitumor effects than Thio-Dam compared to the control group.

4.2 Interpretation of results in the study

Although tumors are diverse and heterogeneous, they all can proliferate beyond the limitations that restrict growth in normal tissue. This ability is what gives tumors their distinguishing characteristic. Together, dysregulated cell proliferation and inhibited apoptosis make up the minimal common platform upon which all neoplastic progression takes place(33). In this investigation, the antiproliferative properties of Thio-Iva and Thio-Dam were demonstrated to target HCC cell lines and more effect than sorafenib. Real-time proliferation experiment revealed a short-term inhibition of both compounds, whilst colony formation assays revealed a long-term inhibition. And has shown good

antineoplastic effects *in vivo*, in addition, the effects of the compounds were not dependent on nonspecific cytotoxicity.

The processes of cell proliferation, differentiation, and death are essential to the functioning of multicellular organisms. There is some evidence to suggest that apoptosis and proliferation are intimately connected(34,35). One of the primary reasons for uncontrolled cell development is that cells can avoid the death process known as apoptosis(36). Next, the study examined whether our inhibitors induce apoptosis. The caspase family is an important molecular group in apoptosis(37). By cleaving target proteins, caspase family proteases regulate cellular pathways(30). Caspase-3 is a member of the cysteine protease family, a crucial enzyme in apoptosis, and is active only after cleavage by cysteinases during apoptosis(31,38). As a result, caspase-3 was selected as the main molecule for detecting apoptosis. Thio-Iva and Thio-Dam treatments boosted caspase-3 activity in a dose- and time-dependent, even more than sorafenib. Active caspases generate a proteolytic cascade capable of cleaving and activating certain substrates, such as poly (ADP-ribose) polymerase (PARP), an enzyme involved in DNA repair and genomic maintenance, and DNA fragmentation factor (39). PARP was reduced and cleaved to an N-terminal 89 kDa fragment, as determined by Western blotting. ROS serve critical functions in controlling DNA damage, apoptosis, cell proliferation, signal transduction, and cell cycle progression. At greater ROS levels, may release ROS that destroys mitochondria and, if it spreads from one mitochondrion to the other, the cell death itself(40). In this work, Thio-Iva and Thio-Dam were found to significantly increase cytoplasmic ROS levels. It can therefore be inferred that acute production of ROS in mitochondria induced by Thio-Iva and Thio-Dam results in apoptosis and subsequent activation of caspase-3.

Elevated ROS levels cause not only mitochondrial damage, which causes cell death, but also DNA damage, which causes cell cycle growth arrest(40). Evidence has found that cyclin B1 is overexpressed in some types of tumors, and cyclin B1 overexpression is positively correlated with cell proliferation, invasion and apoptosis(41). The Western Blot results revealed a decrease in cyclin B1 following Thio-Iva and Thio-Dam treatment, and a strong G2/M phase cell cycle arrest by flow cytometry, implying that the compounds cause cell cycle arrest by inhibiting cyclin B1.

HCC is widely recognized as a highly vascularized tumor. By angiography and imaging, the many and tortuous vascular signs distinguish HCC from benign lesions(42). VEGF is a key angiogenic cytokine that plays a crucial function in tumor angiogenesis. The

production of VEGF was associated with the proliferation of hepatic cells and HCC cells during hepatocarcinogenesis, as well as microvessel invasion and numerous tumor nodules(43). Chemotherapy is of little utility in the treatment of HCC tumor cells due to their genetic variability, and all systemic medicines now approved worldwide are molecularly targeted, with the major mechanism being anti-angiogenesis targeting VEGF and its receptors(22,44). In this study, Thio-Iva and Thio-Dam were described as novel multi-tyrosine kinase inhibitors with VEGFR-2 inhibition, and *in vivo* and *in vitro* investigations verified their anti-angiogenic activities. And in one investigation, NADPH oxidase (Nox) activity downstream of VEGFR-2 activation increased ROS(45). This may be associated with the previous observation of an increase in ROS.

VEGF has also been demonstrated to promote cell mitogenesis, migration, and invasion(46). Activated metastasis and migration is a key feature to distinguishes cancer cells from other cells. Migration is a prerequisite step for metastasis. Thio-Iva and Thio-Dam are described as novel multi-tyrosine kinase inhibitors with VEGFR-2. Result showed Thio-Iva and Thio-Dam can decrease the migration rate both *in vitro*. In addition, both compounds inhibit the growth of HCC tumors grown on CAM which confirm the antineoplastic effect *in vivo*.

4.3 Multi-tyrosine kinase inhibitor in the treatment of HCC

Sorafenib, a multi-tyrosine kinase inhibitor (VEGFR1, 2, and 3; PDGFR; and KIT)(11), was the first molecularly targeted medicine approved for the treatment of hepatocellular carcinoma due to the success of the SHARP and Asia-Pacific trials(47). Through inhibition of the MAP kinase cascade, it can suppress tumor angiogenesis, cell division, and proliferation, and induce apoptosis in cancer cells(48). Although several trials comparing these new medications (sunitinib, brivanib, cediranib, linifanib, and dovotinib) have been conducted, none of them have demonstrated superiority over sorafenib.

After that, almost all the trials were based around sorafenib, and it was used as a control to compare and evaluate novel first-line treatments to improve the prognosis of patients who with HCC. Furthermore, all approved second-line treatments were established on studies comparing sorafenib to placebo(10,49). Newer treatments were ineffective and did not lead to any increased treatment effect until the advent of Lenvatinib(12) in August 2018, which was approved on the basis of non-inferiority to sorafenib. This approval came

after a period of a decade during which sorafenib was the only treatment that had been approved by the FDA for treatment. Even though immunotherapy-based treatments have changed greatly in recent years, the CheckMate-459 study indicated a strong trend toward improved median overall survival (mOS) in patients treated with nivolumab or sorafenib. However, the study did not demonstrate that immunotherapy is superior to sorafenib(20). Because Sorafenib was employed as the standard of therapy, it was used as a control for analysis in this study.

4.4 Strengths and weaknesses of the study

Tyrosine kinases are essential therapeutic targets due to the complex molecular pathogenesis of hepatocellular carcinoma. Although sorafenib for patients with intermediate to advanced HCC has remained stable for more than a decade, the clinical benefit however remains modest, and with drug resistance and intolerance. *In vivo* and *in vitro*, the novel compounds Thio-Iva and Thio-Dam performed better than sorafenib in this investigation. And no significant non-specific cytotoxicity was observed in LDH release assays, nor was there any embryonic toxicity or developmental delay in CAM experiments. Clearly, our medicine had superior results. However, our experiments have only been validated in cell lines and CAM assays. So, the study is only preclinical, next should check out the safety and suitability in respective animal models. Furthermore, the direct mechanism through which these compounds are utilized to treat hepatocellular carcinoma is unknown. So more in-depth research is required.

4.5 Implications for practice and future research

Since 2017, more systemic drugs for advanced stage HCC have been approved for clinical use. The increased number of therapy options may benefit a considerable number of HCC patients who are not acceptable to receive radical treatment. However, many drugs targeting different pathways for systemic medical treatment only showed minimal improvements(49). Therefore, more therapeutic targets are needed and hopefully our tyrosine kinase inhibitors with antiangiogenic and antineoplastic properties will full fill this opening. In the future, combination therapies with other molecular targeted agents or immune checkpoint inhibitors can also be performed to see if there were any addictive or synergistic effects to target HCC. Besides, the usage of Thio-Iva and Thio-Dam in the application to other type of cancer could also be explored.

5 Conclusions

In conclusion, two novel thienyl-based tyrosine kinase inhibitors Thio-Iva and Thio-Dam showed a pronounced effect of antiproliferation, induction of apoptosis, anti-migration, and inhibition of cell cycle effects in HCC cells. Moreover, both compounds indicated antiangiogenic and antineoplastic properties both *in vitro* and *in vivo*. Compared with Thio-Dam, Thio-Iva showed a better overall effect, and both compounds have a superior antiangiogenic and antineoplastic effects compared with clinically relevant HCC therapeutic Sorafenib. However, further investigation on the modes of action of each compound and safety and efficacy evaluation on animal models and are still urgently warranted before they can enter the clinical practice.

Reference list

1. Sung H, Ferlay J, Siegel RL, Laversanne M, Soerjomataram I, Jemal A, Bray F. Global Cancer Statistics 2020: GLOBOCAN Estimates of Incidence and Mortality Worldwide for 36 Cancers in 185 Countries. CA Cancer J Clin. 2021;71(3):209‑49.

2. Ganesan P, Kulik LM. Hepatocellular Carcinoma: New Developments. Clin Liver Dis. 2023;27(1):85-102.

3. Forner A, Díaz-González Á, Liccioni A, Vilana R. Prognosis prediction and staging. Best Pract Res Clin Gastroenterol. 2014;28(5):855‑65.

4. Llovet J, Brú C, Bruix J. Prognosis of Hepatocellular Carcinoma: The BCLC Staging Classification. Semin Liver Dis. 1999;19(03):329‑38.

5. Forner A, Reig M, Bruix J. Hepatocellular carcinoma. The Lancet. 2018;391(10127):1301‑14.

6. Bruix J, Reig M, Sherman M. Evidence-Based Diagnosis, Staging, and Treatment of Patients With Hepatocellular Carcinoma. Gastroenterology. 2016;150(4):835‑53.

7. Reig M, Forner A, Rimola J, Ferrer-Fàbrega J, Burrel M, Garcia-Criado Á, Kelley RK, Galle PR, Mazzaferro V, Salem R, Sangro B, Singal AG, Vogel A, Fuster J, Ayuso C, Bruix J. BCLC strategy for prognosis prediction and treatment recommendation: The 2022 update. J Hepatol. 2022;76(3):681‑93.

8. Cucchetti A, Piscaglia F, Cescon M, Colecchia A, Ercolani G, Bolondi L, Pinna AD. Cost-effectiveness of hepatic resection versus percutaneous radiofrequency ablation for early hepatocellular carcinoma. J Hepatol. 2013;59(2):300‑7.

9. Doyle A, Gorgen A, Muaddi H, Aravinthan AD, Issachar A, Mironov O, Zhang W, Kachura J, Beecroft R, Cleary SP, Ghanekar A, Greig PD, McGilvray ID, Selzner M, Cattral MS, Grant DR, Lilly LB, Selzner N, Renner EL, Sherman M, Sapisochin G. Outcomes of radiofrequency ablation as first-line therapy for hepatocellular carcinoma less than 3 cm in potentially transplantable patients. J Hepatol. 2019;70(5):866‑73.

10. Bruix J, Chan SL, Galle PR, Rimassa L, Sangro B. Systemic treatment of hepatocellular carcinoma: An EASL position paper. J Hepatol. 2021;75(4):960‑74.

11. Llovet JM, Hilgard P, de Oliveira AC, Forner A, Zeuzem S, Galle PR. Sorafenib in Advanced Hepatocellular Carcinoma. N Engl J Med. 2008; 359:378-390.

12. Kudo M, Finn RS, Qin S, Han KH, Ikeda K, Piscaglia F, Baron A, Park JW, Han G, Jassem J, Blanc JF, Vogel A, Komov D, Evans TRJ, Lopez C, Dutcus C, Guo M, Saito K, Kraljevic S, Tamai T, Ren M, Cheng AL. Lenvatinib versus sorafenib in first-line treatment of patients with unresectable hepatocellular carcinoma: a randomised phase 3 non-inferiority trial. The Lancet. 2018;391(10126):1163‑73.

13. Bruix J, Qin S, Merle P, Granito A, Huang YH, Bodoky G, Pracht M, Yokosuka O, Rosmorduc O, Breder V, Gerolami R, Masi G, Ross PJ, Song T, Bronowicki JP, Ollivier-Hourmand I, Kudo M, Cheng AL, Llovet JM, Finn RS, LeBerre MA, Baumhauer A, Meinhardt G, Han G; RESORCE Investigators. Regorafenib for patients with hepatocellular carcinoma who progressed on sorafenib treatment (RESORCE): a randomised, double-blind, placebo-controlled, phase 3 trial. The Lancet. 2017;389(10064):56‑66.

14. Abou-Alfa GK, Meyer T, Cheng AL, El-Khoueiry AB, Rimassa L, Ryoo BY, Cicin I, Merle P, Chen Y, Park JW, Blanc JF, Bolondi L, Klümpen HJ, Chan SL, Zagonel V, Pressiani T, Ryu MH, Venook AP, Hessel C, Borgman-Hagey AE, Schwab G, Kelley RK. Cabozantinib in Patients with Advanced and Progressing Hepatocellular Carcinoma. N Engl J Med. 2018;379(1):54‑63.

15. Yakes FM, Chen J, Tan J, Yamaguchi K, Shi Y, Yu P, Qian F, Chu F, Bentzien F, Cancilla B, Orf J, You A, Laird AD, Engst S, Lee L, Lesch J, Chou YC, Joly AH. Cabozantinib (XL184), a Novel MET and VEGFR2 Inhibitor, Simultaneously Suppresses Metastasis, Angiogenesis, and Tumor Growth. Mol Cancer Ther. 2011;10(12):2298‑308.

16. Zhu AX, Rosmorduc O, Evans TR, Ross PJ, Santoro A, Carrilho FJ, Bruix J, Qin S, Thuluvath PJ, Llovet JM, Leberre MA, Jensen M, Meinhardt G, Kang YK. SEARCH: A Phase III, Randomized, Double-Blind, Placebo-Controlled Trial of Sorafenib Plus

Erlotinib in Patients With Advanced Hepatocellular Carcinoma. J Clin Oncol. 2015;33(6):559‑66.

17. Johnson PJ, Qin S, Park JW, Poon RT, Raoul JL, Philip PA, Hsu CH, Hu TH, Heo J, Xu J, Lu L, Chao Y, Boucher E, Han KH, Paik SW, Robles-Aviña J, Kudo M, Yan L, Sobhonslidsuk A, Komov D, Decaens T, Tak WY, Jeng LB, Liu D, Ezzeddine R, Walters I, Cheng AL. Brivanib Versus Sorafenib As First-Line Therapy in Patients With Unresectable, Advanced Hepatocellular Carcinoma: Results From the Randomized Phase III BRISK-FL Study. J Clin Oncol. 2013;31(28):3517‑24.

18. Cheng A-L, Kang Y-K, Lin D-Y, Park J-W, Kudo M, Qin S, et al. Sunitinib Versus Sorafenib in Advanced Hepatocellular Cancer: Results of a Randomized Phase III Trial. J Clin Oncol. 2013;31(32):4067‑75.

19. Cheng AL, Kang YK, Lin DY, Park JW, Kudo M, Qin S, Chung HC, Song X, Xu J, Poggi G, Omata M, Pitman Lowenthal S, Lanzalone S, Yang L, Lechuga MJ, Raymond E. Comprehensive molecular and immunological characterization of hepatocellular carcinoma. EBioMedicine. 2019; 40:457‑70.

20. Yau T, Park JW, Finn RS, Cheng AL, Mathurin P, Edeline J, Kudo M, Harding JJ, Merle P, Rosmorduc O, Wyrwicz L, Schott E, Choo SP, Kelley RK, Sieghart W, Assenat E, Zaucha R, Furuse J, Abou-Alfa GK, El-Khoueiry AB, Melero I, Begic D, Chen G, Neely J, Wisniewski T, Tschaika M, Sangro B. Nivolumab versus sorafenib in advanced hepatocellular carcinoma (CheckMate 459): a randomised, multicentre, open-label, phase 3 trial. Lancet Oncol. 2022;23(1):77‑90.

21. Avraamides CJ, Garmy-Susini B, Varner JA. Integrins in angiogenesis and lymphangiogenesis. Nat Rev Cancer. 2008;8(8):604‑17.

22. Zhu AX, Duda DG, Sahani DV, Jain RK. HCC and angiogenesis: possible targets and future directions. Nat Rev Clin Oncol. 2011;8(5):292‑301.

23. Apte RS, Chen DS, Ferrara N. VEGF in Signaling and Disease: Beyond Discovery and Development. Cell. 2019;176(6):1248‑64.

24. Zhu AX, Kang YK, Yen CJ, Finn RS, Galle PR, Llovet JM, Assenat E, Brandi G, Pracht M, Lim HY, Rau KM, Motomura K, Ohno I, Merle P, Daniele B, Shin DB, Gerken G, Borg C, Hiriart JB, Okusaka T, Morimoto M, Hsu Y, Abada PB, Kudo M; REACH-2 study investigators. Ramucirumab after sorafenib in patients with advanced hepatocellular carcinoma and increased α-fetoprotein concentrations (REACH-2): a randomised, double-blind, placebo-controlled, phase 3 trial. Lancet Oncol. 2019;20(2):282‑96.

25. Finn RS, Qin S, Ikeda M, Galle PR, Ducreux M, Kim TY, Kudo M, Breder V, Merle P, Kaseb AO, Li D, Verret W, Xu DZ, Hernandez S, Liu J, Huang C, Mulla S, Wang Y, Lim HY, Zhu AX, Cheng AL; IMbrave150 Investigators. Atezolizumab plus Bevacizumab in Unresectable Hepatocellular Carcinoma. N Engl J Med. 2020;382(20):1894‑905.

26. Ma A, Biersack B, Goehringer N, Nitzsche B, Höpfner M. Novel Thienyl-Based Tyrosine Kinase Inhibitors for the Treatment of Hepatocellular Carcinoma. J Pers Med. 2022;12(5):738.

27. Schaller E, Ma A, Gosch LC, Klefenz A, Schaller D, Goehringer N, Kaps L, Schuppan D, Volkamer A, Schobert R, Biersack B, Nitzsche B, Höpfner M. New 3-Aryl-2-(2-thienyl) acrylonitriles with High Activity Against Hepatoma Cells. Int J Mol Sci. 2021;22(5):2243.

28. Guzman C, Bagga M, Kaur A, Westermarck J, Abankwa D. ColonyArea: an ImageJ plugin to automatically quantify colony formation in clonogenic assays. PloS One. Public Library of Science San Francisco, USA; 2014;9(3):e92444.

29. Goehringer N, Biersack B, Peng Y, Schobert R, Herling M, Ma A, Nitzsche B, Höpfner M. Anticancer Activity and Mechanisms of Action of New Chimeric EGFR/HDAC-Inhibitors. Int J Mol Sci. 2021;22(16):8432.

30. Shalini S, Dorstyn L, Dawar S, Kumar S. Old, new and emerging functions of caspases. Cell Death Differ. 2015;22(4):526‑39.

31. Lakhani SA, Masud A, Kuida K, Porter GA Jr, Booth CJ, Mehal WZ, Inayat I, Flavell RA. Caspases 3 and 7: Key Mediators of Mitochondrial Events of Apoptosis. Science. 2006;311(5762):847‑51.

32. Park M, Chae HD, Yun J, Jung M, Kim YS, Kim SH, Han MH, Shin DY. Constitutive activation of cyclin B1-associated cdc2 kinase overrides p53-mediated G2-M arrest. Cancer Res. AACR; 2000;60(3):542‑5.

33. Evan GI, Vousden KH. Proliferation, cell cycle and apoptosis in cancer. nature. Nature Publishing Group; 2001;411(6835):342‑8.

34. Alenzi FQB. Links between apoptosis, proliferation and the cell cycle. Br J Biomed Sci. 2004;61(2):99‑102.

35. Evan GI, Wyllie AH, Gilbert CS, Littlewood TD, Land H, Brooks M, Waters CM, Penn LZ, Hancock DC. Induction of apoptosis in fibroblasts by c-myc protein. Cell. 1992;69(1):119‑28.

36. D'arcy MS. Cell death: a review of the major forms of apoptosis, necrosis and autophagy. Cell Biol Int. Wiley Online Library; 2019;43(6):582‑92.

37. Grütter MG. Caspases: key players in programmed cell death. Curr Opin Struct Biol. 2000;10(6):649‑55.

38. Asadi M, Taghizadeh S, Kaviani E, Vakili O, Taheri-Anganeh M, Tahamtan M, Savardashtaki A. Caspase-3: Structure, function, and biotechnological aspects. Biotechnol Appl Biochem. 2022;69(4):1633‑45.

39. Lin C, Holland RE, Donofrio JC, McCoy MH, Tudor LR, Chambers TM. Caspase activation in equine influenza virus induced apoptotic cell death. Vet Microbiol. 2002;84(4):357‑65.

40. Zorov DB, Juhaszova M, Sollott SJ. Mitochondrial reactive oxygen species (ROS) and ROS-induced ROS release. Physiol Rev. 2014;94(3):909‑50.

41. Tang L, Zhang Y, Pan H, Luo Q, Zhu XM, Dong MY, Leung PC, Sheng JZ, Huang HF. Involvement of cyclin B1 in progesterone-mediated cell growth inhibition, G2/M

cell cycle arrest, and apoptosis in human endometrial cell. Reprod Biol Endocrinol. BioMed Central; 2009;7(1):1‑8.

42. Miller G, Schwartz LH, D'Angelica M. The use of imaging in the diagnosis and staging of hepatobiliary malignancies. Surg Oncol Clin N Am. Elsevier; 2007;16(2):343‑68.

43. Fernández M, Semela D, Bruix J, Colle I, Pinzani M, Bosch J. Angiogenesis in liver disease. J Hepatol. 2009;50(3):604‑20.

44. Zanotelli MR, Reinhart-King CA. Mechanical Forces in Tumor Angiogenesis. Adv Exp Med Biol. 2018; 1092:91‑112.

45. Claesson-Welsh L, Welsh M. VEGFA and tumour angiogenesis. J Intern Med. 2013;273(2):114‑27.

46. Shibuya M, Claesson-Welsh L. Signal transduction by VEGF receptors in regulation of angiogenesis and lymphangiogenesis. Exp Cell Res. Elsevier; 2006;312(5):549‑60.

47. Ranieri G, Gadaleta-Caldarola G, Goffredo V, Patruno R, Mangia A, Rizzo A, Sciorsci RL, Gadaleta CD. Sorafenib (BAY 43-9006) in hepatocellular carcinoma patients: from discovery to clinical development. Curr Med Chem. 2012;19(7):938‑44.

48. Gao J-J, Shi Z-Y, Xia J-F, Inagaki Y, Tang W. Sorafenib-based combined molecule targeting in treatment of hepatocellular carcinoma. World J Gastroenterol. 2015;21(42):12059‑70.

49. Pinter M, Peck-Radosavljevic M. Review article: systemic treatment of hepatocellular carcinoma. Aliment Pharmacol Ther. 2018;48(6):598‑609.

Statutory Declaration

“I, Andi,Ma, by personally signing this document in lieu of an oath, hereby affirm that I prepared the submitted dissertation on the topic [Novel Small Molecules for treatment of hepatocellular cancer / Neuartige kleine Moleküle zur Behandlung von Leberzellkrebs], independently and without the support of third parties, and that I used no other sources and aids than those stated.
All parts which are based on the publications or presentations of other authors, either in letter or in spirit, are specified as such in accordance with the citing guidelines. The sections on methodology (in particular regarding practical work, laboratory regulations, statistical processing) and results (in particular regarding figures, charts and tables) are exclusively my responsibility.

Furthermore, I declare that I have correctly marked all of the data, the analyses, and the conclusions generated from data obtained in collaboration with other persons, and that I have correctly marked my own contribution and the contributions of other persons (cf. declaration of contribution). I have correctly marked all texts or parts of texts that were generated in collaboration with other persons.

My contributions to any publications to this dissertation correspond to those stated in the below joint declaration made together with the supervisor. All publications created within the scope of the dissertation comply with the guidelines of the ICMJE (International Committee of Medical Journal Editors; http://www.icmje.org) on authorship. In addition, I declare that I shall comply with the regulations of Charité – Universitätsmedizin Berlin on ensuring good scientific practice.

I declare that I have not yet submitted this dissertation in identical or similar form to another Faculty.

The significance of this statutory declaration and the consequences of a false statutory declaration under criminal law (Sections 156, 161 of the German Criminal Code) are known to me.”

Date Signature

Declaration of your own contribution to the publications

Andi Ma contributed the following to the below listed publication:

Publication : **Ma A**, Biersack B, Goehringer N, Nitzsche B, Höpfner M. Novel Thienyl-Based Tyrosine Kinase Inhibitors for the Treatment of Hepatocellular Carcinoma. J Pers Med. 2022;12(5):738.

Contributions (in detail):

Performed and analyzed Determination of IC50 values (Publication: Table 1)

Western blot of inhibition of VEGFR-2 phosphorylation (Publication : Figure 2c-d)

Real-time proliferation detection by iCELLigence (Publication : Figure 3)

In line with the long-time proliferation analysis by clonogenic growth (Publication : Figure 4)

Cytotoxic effects by LDH assay (Publication : Figure 5)

Apoptosis effects with caspase-3 actively test, Western blot, ROS assay (Publication : Figure 6)

Cell cyclin detect by Flow cytometry and Western blot (Publication : Figure 7),

Antimigratory effects by migration assay (Publication : Figure 8),

In vitro and in vivo effects of on angiogenesis by tube formation assay and CAM assay (Publication : Figure 9)

In vivo antineoplastic effects by CAM assay (Publication : Figure 10).

_____

Signature, date and stamp of first supervising university professor / lecturer

_____

Signature of doctoral candidate

Excerpt from Journal Summary List

Journal Data Filtered By: **Selected JCR Year: 2020** Selected Editions: SCIE,SSCI
Selected Categories: **"HEALTH CARE SCIENCES and SERVICES"**
Selected Category Scheme: WoS
Gesamtanzahl: 108 Journale

Rank	Full Journal Title	Total Cites	Journal Impact Factor	Eigenfactor Score
1	npj Digital Medicine	2,406	11.653	0.007450
2	Implementation Science	14,750	7.327	0.020010
3	BMJ Quality & Safety	7,335	7.035	0.014360
4	ACADEMIC MEDICINE	22,828	6.893	0.027600
5	JOURNAL OF CLINICAL EPIDEMIOLOGY	36,224	6.437	0.028360
6	HEALTH AFFAIRS	22,442	6.301	0.047250
7	MEDICAL EDUCATION	14,132	6.251	0.011580
8	JOURNAL OF TELEMEDICINE AND TELECARE	5,052	6.184	0.005600
9	VALUE IN HEALTH	12,642	5.725	0.017860
10	JOURNAL OF MEDICAL INTERNET RESEARCH	26,102	5.428	0.039100
11	JOURNAL OF GENERAL INTERNAL MEDICINE	26,727	5.128	0.028950
12	International Journal of Integrated Care	2,034	5.120	0.002800
13	International Journal of Health Policy and Management	2,118	5.007	0.005600
14	PHARMACOECONOMICS	6,543	4.981	0.009170
15	Journal of Personalized Medicine	1,071	4.945	0.002290
16	MILBANK QUARTERLY	4,632	4.911	0.005270
17	JMIR mHealth and uHealth	7,694	4.773	0.015520
18	PALLIATIVE MEDICINE	7,332	4.762	0.009100
19	BMC Medical Research Methodology	16,557	4.615	0.017550

Printing copy of the publication

Journal of *Personalized Medicine*

MDPI

Article

Novel Thienyl-Based Tyrosine Kinase Inhibitors for the Treatment of Hepatocellular Carcinoma

Andi Ma [1], Bernhard Biersack [2], Nils Goehringer [1], Bianca Nitzsche [1,*] and Michael Höpfner [1]

[1] Institute of Physiology, Charité—Universitätsmedizin Berlin, Corporate Member of Freie Universität Berlin, Humboldt-Universität zu Berlin and Berlin Institute of Health, 10117 Berlin, Germany; andi.ma@charite.de (A.M.); nils.goehringer@charite.de (N.G.); michael.hoepfner@charite.de (M.H.)
[2] Organic Chemistry 1, University of Bayreuth, Universitätsstrasse 30, 95440 Bayreuth, Germany; bernhard.biersack@uni-bayreuth.de
* Correspondence: bianca.nitzsche@charite.de

Abstract: New medical treatments are urgently needed for advanced hepatocellular carcinoma (HCC). Recently, we showed the anticancer effects of novel thiophene-based kinase inhibitors. In this study, we further characterized the antineoplastic effects and modes of action of the two most promising inhibitors, Thio-Iva and Thio-Dam, and compared their effects with the clinically relevant multi-kinase inhibitor, sorafenib, in HCC cells. Crystal violet staining and real-time cell growth monitoring showed pronounced antiproliferative effects in Huh-7 and SNU-449 cells with IC_{50} values in the (sub-)micromolar range. Long-term incubation experiments revealed the reduced clonogenicity of Thio-Iva and Thio-Dam-treated HCC cells. LDH-release tests excluded cytotoxicity as an unspecific mode of action of the inhibitors, while flow cytometry analysis revealed a dose-dependent and pronounced G2/M phase cell cycle arrest and cyclin B1 suppression. Additionally, mitochondria-driven apoptosis was observed through the cytosolic increase of reactive oxygen species, a concomitant PARP cleavage, and caspase-3 induction. Both compounds were found to effectively inhibit the capillary tube formation of endothelial EA.hy926 cells in vitro, pointing towards additional antiangiogenic effects. Antiangiogenic and antineoplastic effects were confirmed in vivo by CAM assays. In summary, the thienyl-acrylonitrile derivatives, Thio-Iva and Thio-Dam, exert significant antineoplastic and antiangiogenic effects in HCC cells.

Keywords: hepatocellular carcinoma; anticancer drugs; treatment; angiogenesis; multi-kinase inhibitor

Citation: Ma, A.; Biersack, B.; Goehringer, N.; Nitzsche, B.; Höpfner, M. Novel Thienyl-Based Tyrosine Kinase Inhibitors for the Treatment of Hepatocellular Carcinoma. *J. Pers. Med.* **2022**, *12*, 738. https://doi.org/10.3390/jpm12050738

Academic Editor: Diego F. Calvisi

Received: 5 April 2022
Accepted: 28 April 2022
Published: 1 May 2022

1. Introduction

Hepatocellular carcinoma (HCC) is the sixth most common cancer in the world [1]. HCC emerges in patients with chronic liver inflammation associated with viral infection, alcohol abuse, or metabolic syndrome. Its incidence is constantly rising, and the relative 5-year survival rate is below 20%. At present, the clinical treatment options for early-stage HCC include surgical resection, liver transplantation, or percutaneous ablation [3]. However, as most patients are already in an advanced disease stage when diagnosed, these radical treatment options are often not applicable. For patients with advanced HCC, palliative therapy by trans-arterial chemoembolization or systemic therapy with tyrosine kinase inhibitors such as sorafenib are methods of choice. However, tumor growth control, relieve of disease-related symptoms, and the overall survival of sorafenib-treated patients with advanced HCC is not convincingly improved and is hampered by the occurrence of resistance to sorafenib treatment [4]. Thus far, no effective medical treatment exists for patients suffering from advanced HCC, emphasizing the urgent need for new and efficient therapeutic agents for HCC treatment.

Key enzymes of cellular signal transduction pathways correlated with tumor cell differentiation and proliferation are valuable targets for anticancer drug screening leading

to the development of new drug candidates with high efficiency, low toxicity, and high specificity [5].

Sorafenib is a prominent clinically approved example of a small molecule multi-kinase inhibitor, which targets vascular endothelial growth factor receptors (VEGFR) 1–3, platelet-derived growth factor receptor-β (PDGFR-β), and rapidly accelerated fibrosarcoma kinases (Raf kinases) [6]. Sorafenib was the only first-line systemic targeted drug available for advanced HCC for almost one decade, with a survival benefit of three months [7].

However, clinical studies have reported that a considerable proportion of HCC patients does not respond to sorafenib treatment. The response rate to sorafenib is less than 50%, and most patients develop disease progression within six months [8,9]. Due to the early occurrence of sorafenib resistance, most patients do not have long-term benefits, and thus the overall efficacy of sorafenib is far from satisfactory. Over the last years, further first-line and second-line therapies which are based on the receptor tyrosine kinase inhibitors regorafenib, lenvatinib, or ramucirumab have emerged [10–12]. Immunotherapy is a relatively new field of HCC research. The majority of HCCs arise from chronic liver disease where T cells are constantly exposed to antigen and inflammatory signals. This condition induces a state of upregulated receptors, such as the programmed cell death protein-1 (PD-1). The PD-1 inhibitor nivolumab was approved in 2017 as a second-line treatment for advanced HCC but failed to show statistically significant benefits over sorafenib such as being progression-free and improved overall survival rates [13]. These drawbacks of HCC immunotherapies necessitate stronger efforts in the search for new drugs against HCC.

Tumor angiogenesis plays a vital role in the growth and dissemination of solid tumors. Hypervascularity and marked vascular abnormalities such as arterialization and sinusoidal capillarization are common tumor-associated features of HCC [14]. Vascular endothelial growth factors (VEGFs, e.g., VEGF-A, VEGF-B, VEGF-C, VEGF-D) and the receptor tyrosine kinases (RTKs) VEGFR-1, VEGFR-2, and VEGFR-3 are crucial for the promotion of tumor angiogenesis [15,16]. Tumor-induced angiogenesis is based on two mechanisms, i.e., the overexpression of angiogenic factors and the inhibition of anti-angiogenic factors, which lead to the enhanced development of blood vessels lacking in normal vascular structures with regulated blood vessel diameter and tissue-related perfusion. Antiangiogenic therapy based on antibodies and small-molecule VEGFR inhibitors was developed to inhibit the growth and further spreading of abnormal tumor blood vessels that lead to tumor hypoxia and shrinkage [17,18].

Various reports have described the promising anti-tumor activities of thiophene-based compounds [19,20]. Recently, we identified some *E*-2-(2-thienyl)-3-acrylonitrile derivatives with high anti-tumor efficacy in p53 wild-type HepG2 hepatoblastoma cells which were more active than the clinically applied multi-kinase inhibitor sorafenib [21]. These compounds are likewise multi-kinase inhibitors with preferential activity against VEGFR-2. In this work, we further analyzed the mode of action of these promising compounds (Figure 1) in HCC cells.

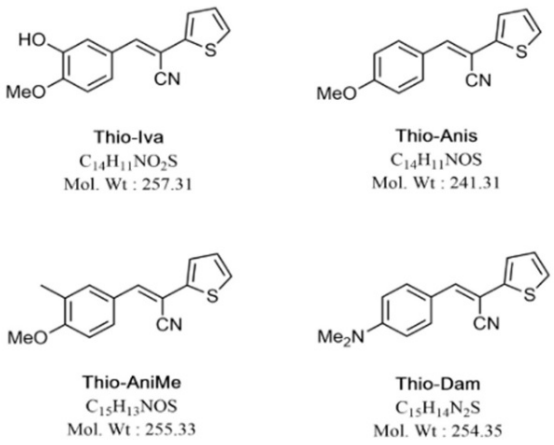

Figure 1. Chemical structures of E-2-(2-thienyl)-3-acrylonitrile RTK inhibitors used in this study.

2. Materials and Methods

2.1. Compounds

Stock solutions (10 mM) of Thio-Iva, Thio-Dam, Thio-Anis, Thio-Anime, and sorafenib were prepared in dimethyl sulfoxide (DMSO Thermo Fisher Scientific, Inc., Waltham, Ma, USA) and stored at −20 °C. Sorafenib was purchased from Targetmol (T0093L, Boston, MA, USA). Thio-Iva, Thio-Dam, Thio-Anis, and Thio-Anime were synthesized and provided by Dr. Biersack (Dept. of Organic Chemistry, University of Bayreuth, Bayreuth, Germany) [21].

2.2. Biological Evaluation

2.2.1. Cell Culture

Highly differentiated and p53-mutated Huh-7 (JCRB#0403) human hepatocellular carcinoma cells were grown in RPMI 1640 medium supplemented with 10% fetal bovine serum, 100 U/mL penicillin, and 100 mg/mL streptomycin (all from Gibco, Thermo Fisher Scientific, Inc., Waltham, Ma, USA). The p53-mutated SNU-449 cells (ATCC#2234) were grown in RPMI 1640 medium supplemented with 10% fetal bovine serum, 100 U/mL penicillin, 100 mg/mL streptomycin, 1%HEPES, and 1% sodium pyruvate. EA.hy926 human umbilical vein cells were grown in DMEM containing 10% fetal bovine serum, 100 U/mL penicillin, and 100 mg/mL streptomycin. All cells were incubated at 37 °C, 5% CO_2, 95% humidified atmosphere.

2.2.2. Crystal Violet Staining

The treatment-induced inhibition of cell proliferation was assessed using crystal violet staining, as described earlier [22]. In brief, 1500 cells/well seeded in 96-well plates were allowed to adhere to the bottom of the wells for 72 h. Thereafter, the cells were incubated with rising concentrations (0.1–20 µM) of each test compound for up to 48 h. After that, cells were rinsed with PBS, fixed with 1% glutaraldehyde, and 0.1% crystal violet (N-hexamethylpararosaniline, Sigma Aldrich) was added to stain the cells. Unbound dye was removed by rinsing with water. The cell-bound crystal violet was dissolved using 0.2% Triton X-100 (Sigma-Aldrich, Munich, Germany). The extinction of crystal violet, which increases linearly with the increase of the cell number, was measured with an ELISA-Reader (Dynex Technologies, Denkendorf, Germany) at 570 nm [23].

2.2.3. Real-Time Monitoring of Cell Proliferation

The real-time cell analyzer iCELLigence system (ACEA Biosciences San Diego, CA, USA) was used to monitor cell proliferation and survival, as previously described [24]. Cells were seeded in 8-well micro-E-plates (ACEA Biosciences, San Diego, CA, USA) at a

density of 6000 cells/well. Incubation for 24 h allowed for attachment, and the medium was replaced thereafter by Thio-Iva or Thio-Dam-containing medium in rising concentrations (0.1–10 μM). The impedance-based iCELLigence system determined proliferation by measuring changes in the electrical resistance of the bottom of each well every 15 min, for up to 96 h. Electrical resistance increases when the number of attached cells increases due to mitosis. Data are recorded as a unitless parameter called cell index, which is defined as $(R_{tn}–R_{t0})/4.6$ Ohm, with R_{tn} being the measured resistance at time point n and R_{t0} being background resistance measured at time point T0.

2.2.4. Colony Formation Assay

The proliferation of long-term effects was assessed by colony formation assays. Cells were seeded in 6-well plates at a density of 300 cells/well, and colony formation and growth were observed for 2 weeks [21]. Then, the colonies were washed twice with PBS and fixed with 4% formaldehyde for 1 h before staining with 0.5% crystal violet for 3 min. A colony was defined as a cell aggregate with 50 or more cells [21], and so only colonies with 50 or more cells were counted. Representative images were taken by a kappa digital camera system (Kappa Optronics GmbH, Gleichen, Germany). Stained colonies were quantified using the Colony Area ImageJ plug-in application (Vision 1.52a, National Institutes of Health, USA).

2.2.5. Enzymatic Kinase Assay

A cell-free kinase assay consisting of a custom panel of 32 protein kinases involved in cell proliferation and angiogenesis was used to screen the kinase-inhibiting potency of Thio-Iva (10 μM). The assay was performed by Eurofins Kinase Profiler TM service (Eurofins, Celle-Lévescault, France), and the determination of enzymatic activity was assessed as previously described [21]. Moreover, a dose-response curve for Thio-Iva (0.003–30 μM) was executed to determine the IC_{50} of Thio-Iva-induced VEGFR-2 inhibition.

2.2.6. Determination of Caspase-3

Caspase-3 activity was measured to determine Thio-Iva and Thio-Dam-induced apoptosis in HCC cells [25]. A total of 100,000 cells/well were seeded in 6-well plates and maintained for 24 h. Thereafter, the cells were incubated with 1 μM and 10 μM of each test compound for 24 h and 48 h, respectively. After that, the cells were collected and lysed using lysis buffer at 4 °C for 30 min. The protein content of the samples was quantified using Pierce™ BCA Protein Assay Kit (Thermo Fisher Scientific) to adjust equal amounts of protein for the following caspase-3 determination. The samples were incubated with AC-DEVD-AMC (EMD Millipore, Billerica, MA, USA) at 37 °C for 1 h. Active caspase-3 cleaved AC-DEVD-AMC to produce fluorescent AC-DEVD, which was measured using a VarioSkan Flash 40053 microplate luminometer (Thermo Fisher Scientific, Waltham, MA, USA; filter sets: e.g., 360/40 nm, em 460/10 nm) [21].

2.2.7. Determination of Compound-Induced Cytotoxicity

Cytotoxicity was quantified with a KitPLUS lactate dehydrogenase (LDH) assay (Roche Diagnostics GmbH, Mannheim, Germany). A total of 4×10^4 cells/well were seeded in 96-well plates for 24 h and then incubated with 1 μM and 10 μM of Thio-Iva and Thio-Dam for 6 h and 24 h. Supernatant was collected for LDH determination according to the manufacturer's instructions. Then, 100 μL of a mixture of catalyst and dye solution was added, and cells were incubated for a maximum of 30 min. LDH can catalyze the synthesis of pyruvate from lactic acid, and then the reaction of pyruvate to 2,4-dinitrophenylhydrazine, which forms a brownish red solution under basic conditions. An ELISA reader (Dynex Technologies, Denkendorf, Germany) was used at 490/630 nm for the measurement of cytotoxicity indicating the leakage of LDH into the supernatant of the cells. Data are expressed as the percentage (%) of the total LDH activity (LDH in the

medium + LDH in the cell), according to the equation % LDH released = (LDH activity in the medium/total LDH activity) × 100 [23].

2.2.8. Scratch Assay

Cells (1.5×10^5 cells/well) were seeded in 6-well pates and allowed to grow to (sub-) confluence. Using a 10 µL pipette tip, the cell monolayer was scratched vertically. The cells on the edge of this artificial gap migrate into the cell-free area to close the gap in a time-dependent manner. The cells were rinsed with PBS, and fresh medium was added, which contained rising concentrations of Thio-Iva and Thio-Dam (1–10 µM), and a corresponding volume of DMSO was used for control. The cells were incubated for 24 h (37 °C, 5% CO_2, 95% humidity), followed by photographical documentation with an EVOS M5000 microscope (Thermo Fischer Scientific, Waltham, MA, USA). The migration of cells was quantified using the TScratch software (https://github.com/cselab/TScratch, accessed on 5 April 2022; CSElab, Zurich, Swiss). Migration values were normalized to control, which was set as 100% [25].

2.2.9. Measurement of Reactive Oxygen Species (ROS)

The formation of cytosolic ROS was performed as described [26]. Measurement was performed by using the membrane-permeable dye CellROX® Orange (Thermo Fisher Scientific, Inc., Waltham, Ma, USA), which accumulates in the cytoplasm and exhibits a strong fluorescent signal upon oxidation at excitation/emission levels of 545 nm/565 nm [26]. CellROX® Orange reagent (1 µM) was applied together with Thio-Iva (1 and 10 µM) and Thio-Dam (1 and 10 µM). Cells incubated with 1.6 mM H_2O_2 for 30 min served as positive controls. Formation of ROS was measured after 24 h of incubation with the compounds using a ZOE™ Fluorescent Cell Imager (Biorad, Munich, Germany).

2.2.10. Cell-Cycle Analysis by Flow Cytometry

Flow cytometry was applied for cell cycle analysis by staining the DNA of treated HCC cells with propidium iodide (PI) nucleic acid stain (Invitrogen, Eugene, OR, USA). Huh-7 and SNU-449 cells were seeded in 6-well plates with a density of 20,000 cells/mL and treated with different concentrations of Thio-Iva and Thio-Dam for 48 h. Then, the cells were harvested and fixed in 70% ethanol overnight and incubated with RNaseA (0.4 mg/mL) in PBS at 37 °C for 30 min. PI was added and cells were incubated for 30 min in the dark. Samples were analyzed using FACSCanto II (BD Biosciences, Heidelberg, Germany). Data analysis was done with FlowJo 10.4 software (LLC, Ashland, OR, USA).

2.2.11. Tube Formation

A total of 50 µL of cold Matrigel/well (Corning™ 354234, Tewksbury, MA, USA) was plated out in a 4 °C cold 96-well plate and allowed to polymerize in a 37 °C incubator for 2 h. Then, EA.hy926 cells were suspended in DMEM containing different concentrations of Thio-Iva and Thio-Dam and inoculated to the Matrigel at a density of 2500 cells/well. After incubation at 37 °C and 5% CO_2 for 6 h, photographical documentation was executed with an EVOS M5000 microscope (Thermo Fischer Scientific, Waltham, MA, USA). For the analysis and quantification of tube formation, the Angiogenesis Analyzer plugin of ImageJ (NIH, Bethesda, MD, USA) was employed. Results are expressed as total segment length.

2.2.12. Western Blot

Western blotting was performed as described previously [27]. In short, radioimmunoprecipitation assay (RIPA) buffer was used to lyse whole-cell extracts. Protein was quantified by the bicinchoninic acid (BCA) assay. An equal amount of protein (20 µL) was separated from each sample by sodium dodecyl sulfate-polyacrylamide gel electrophoresis and transferred to a polyvinylidene fluoride membrane (PVDF), followed by incubation with primary antibody overnight at 4 °C. Antibodies of phospho-VEGF Receptor2 (#3817 Cell Signaling Technology, Danvers, MA, USA, 1:500), cyclin B1 (sc-245 Santa Cruz Biotech-

nology, Santa Cruz, CA, USA, 1:1000), poly-(ADP-ribose)-polymerase (PARP) and cleaved PARP (11835238 Roche Mannheim, Germany, 1:1000), and β-actin (A5441 Sigma Aldrich, Taufkirchen, Germany, 1:2000) were used. Then, incubation with the corresponding anti-mouse (NA931VS Santa Cruz Biotechnology, 1:10,000) or anti-rabbit (NA934VS Santa Cruz Biotechnology, 1:10,000) peroxidase-coupled anti-IgG secondary antibodies was carried out at room temperature for a minimum of 1 h. Subsequently, antibody bondage was illustrated using Clarity Max ECL Western Blotting Substrates (Biorad, Munich, Germany) for detection and Celvin-S developer (Biostep, software SnapAndGo, Burkhardtsdorf, Germany) for development.

2.2.13. Chicken Chorioallantoic Membrane Assay (CAM)

In vivo assays employing the chorioallantoic membrane (CAM) of fertilized chicken eggs were performed to test the anti-neoplastic and anti-angiogenic effects of the novel compounds, as described previously [21]. In short, fertilized chicken eggs (Gallus gallus) were obtained from a commercial provider (Valo Biomedia GmbH, Osterholz-Scharmbeck, Germany), and the development was induced by incubating the eggs at a temperature of 37.8 °C with 66% relative humidity. On day 3, the eggs were opened by cutting the shell at the top part of the egg.

For anti-angiogenesis testing, a silicone ring (diameter: 5 mm) was placed on the CAM for 24 h to be able to stably connect the ring to the CAM. On day 12, 20 µL of test compounds (0.2, 0.5, 1.0 µM) diluted with 0.9% NaCl was pipetted into the ring. The blood vessel status of the CAM was documented after 48 h by using a digital camera (Distelkamp-Electronic, Kaiserslautern, Germany). The degree of angiogenesis was quantified by measuring the length of the blood vessels using Image Pro Plus 6.0 (Image-pro Plus, Media Cybernetics, Inc., Silver Spring, MD, USA).

For anti-neoplastic testing, a total of 3×10^6 Huh-7 cells were resuspended in 10 µL cell culture media and 10 µL Matrigel (Corning™ 354234, MA, Tewksbury, USA) (BD Biosciences) before the cell suspension was applied to a silicone ring (5 mm in diameter) on the CAM of fertilized chicken eggs on day 8 of their embryonic development. The tumor-bearing chicken eggs were incubated for 24 h at 37.8 °C to stimulate tumor formation, followed by the topical application of 20 µL medium containing Thio-Iva, Thio-Dam, or sorafenib. After an incubation period of 72 h at 37.8 °C and 66% humidity, the tumors were excised and carefully weighed to determine their mass.

2.2.14. Statistical Analysis

GraphPad (version 8.00, San Diego, CA, USA) was used for statistical analysis. Unless otherwise specified, all experiments were independently repeated for 3–5 times, and the results are expressed as means ± SD or SEM, respectively. Statistical significance was calculated by performing a one-way analysis of variance (ANOVA).

3. Results

3.1. Biological Evaluation

3.1.1. IC_{50} Determination of Novel Thiophene-Based Compounds in HCC Cells

The crystal violet staining method was used to determine the growth inhibitory effects of the four thiophene-based test compounds on the two human HCC cell lines, Huh-7 and SNU-449. Thio-Iva showed the highest activities, with IC_{50} values of 0.29 ± 0.18 µM (Huh-7) and 0.53 ± 0.32 µM (SNU-449) after 48 h of treatment. Thio-Dam also showed considerable antiproliferative activity, with IC_{50} values of 0.81 ± 0.26 µM and 1.64 ± 0.51 µM, respectively, and thus, both Thio-Iva and Thio-Dam were distinctly more active than the clinically approved VEGFR inhibitor sorafenib (IC_{50} = 2.50 ± 0.14 µM for Huh-7 and >8 µM for SNU-449) (Table 1). The closely related derivatives Thio-Anis and Thio-AniMe were also slightly more active against Huh-7 cells than sorafenib. However, in the SNU-449 cells, Thio-Anis, Thio-AniMe, and sorafenib were distinctly less active and did not show pronounced

antiproliferative activity at doses of 8 μM and higher. Thus, for further evaluations, only the two best working compounds, Thio-Iva, and Thio-Dam, were chosen.

Table 1. Determination of IC_{50} values (μM) of test compounds for the Huh-7 and SNU-449 HCC cell lines after incubation for 48 h.

Compounds	Huh-7	SNU-449
Thio-Iva	0.29 ± 0.18	0.53 ± 0.32
Thio-Dam	0.81 ± 0.26	1.64 ± 0.51
Thio-Anis	1.20 ± 0.42	>8
Thio-AniMe	1.85 ± 0.21	>8
Sorafenib	2.50 ± 0.14	>8

3.1.2. Kinase Inhibitory Effects of Thio-Iva and Thio-Dam

A cell-free kinase assay was used to screen for the kinase inhibitory potency of the most effective thiophene-based test compound, Thio-Iva, in a customized panel of 32 protein kinases. The kinases were selected because of their relevance to the proliferation and angiogenesis of HCC [21]. Thio-Iva showed multi-kinase inhibitory activity, with the most pronounced effects on VEGFR-2, which was inhibited by ~90% (Figure 2a). In the following step, a dose–response curve was determined for the inhibition of VEGFR-2 by Thio-Iva (0.003–30 μM) (Figure 2b). In the cell-free kinase assay, the IC_{50} value of Thio-Iva amounted to 3.31 μM.

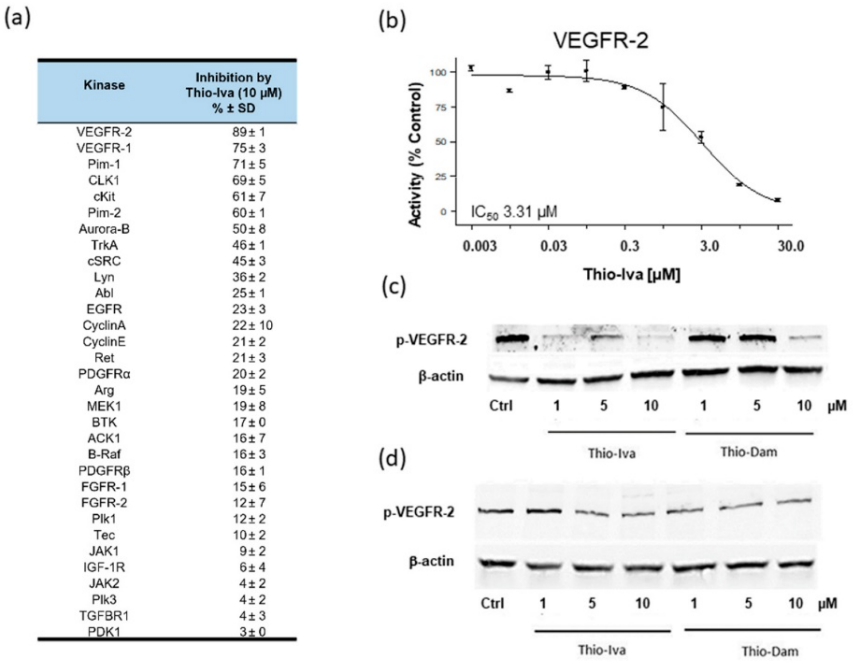

Figure 2. VEGFR-2 inhibition by novel compounds. Enzymatic kinase profiling on 32 kinases revealed multi-kinase inhibition of Thio-Iva, with the most pronounced effects on VEGFR-2 kinase (**a**). Dose–response curve for Thio-Iva-induced VEGFR-2 kinase inhibition (**b**). Data are given as means ± SD of n = 2–3 independent determinations per kinase. Western blot of Thio-Iva and Thio-Dam-induced inhibition of VEGFR-2 phosphorylation in Huh-7 (**c**) and SNU-449 (**d**) cells after 24 h of incubation, confirming the VEGFR-2 inhibiting effects of both compounds on the cellular level.

To confirm VEGFR-2 inhibiting effects on the cellular level, the dephosphorylating effects of Thio-Iva and Thio-Dam were determined in HuH-7 and SNU-449 cells (Figure 2c,d). Both compounds showed a dose-dependent suppression of VEGFR-2 phosphorylation in both cell lines, with Thio-Iva being more effective as compared to Thio-Dam.

3.1.3. Antiproliferative Activity of Thio-Iva and Thio-Dam in HCC Cells

In order to further evaluate the dynamic effects of Thio-Iva and Thio-Dam on the proliferation of HCC, the iCELLigence system monitoring cell proliferation in real time was used. In the control group, both Huh-7 (Figure 3a) and SNU-449 (Figure 3c) cells showed vigorous growth, as shown by the cell index (CI), which continued to increase over time. By contrast, when treated with Thio-Iva or Thio-Dam (0.1–1.0 µM), both cell lines showed a dose-dependent reduction in the increase of the CI values, indicating a dose-dependent reduction of cell proliferation.

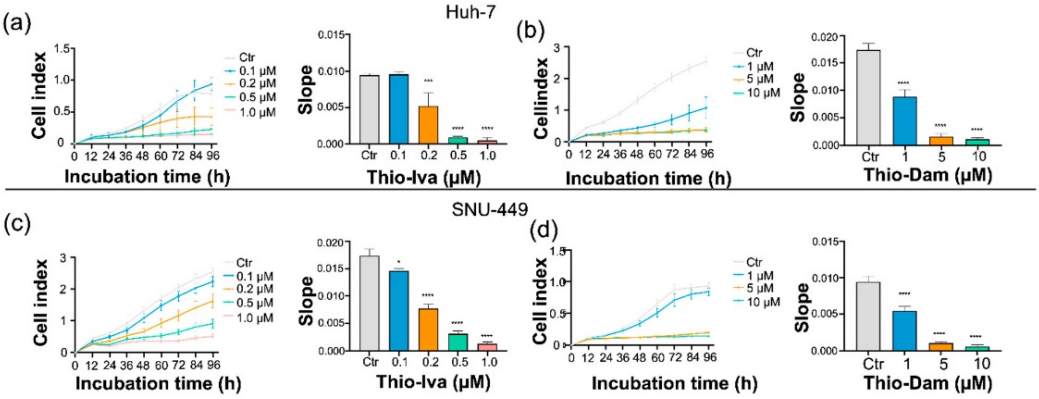

Figure 3. Real-time proliferation detection by iCELLigence. Dose-dependent effects of Thio-Iva and Thio-Dam on the cell index (CI) and its slope over time in Huh-7 (**a**,**b**) and SNU-449 cells (**c**,**d**). Statistical significance * $p < 0.05$, *** $p < 0.001$, and **** $p < 0.0001$ by ordinary one-way ANOVA as compared to untreated control. All results were expressed as means ± SEM of 3 independent experiments.

Calculating the slope of the cell index that reflected the proliferation dynamics over time revealed a dose-dependent and highly significant decline to almost zero which came after incubation with the rising concentrations of Thio-Iva and Thio-Dam, both in Huh-7 (Figure 3b) as well as in SNU-449 (Figure 3d) cells, thus impressively showing the antiproliferative effect of both compounds. Furthermore, the CI graphs also revealed that the onset of Thio-Iva-induced growth inhibition occurred after ~24 h, while that of Thio-Dam had already occurred after only ~12 h.

In line with the iCELLigence proliferation data, long-term surveys (14 days) employing clonogenic assays also yielded a highly significant and dose-dependent reduction in the colony formation of Huh-7 (Figure 4a,b) and SNU-449 (Figure 4c,d) cells by >90% after Thio-Iva (0.1–0.4 µM) and Thio-Dam (0.5–5 µM) treatment, respectively. In both cell models, the anti-clonogenic effects of Thio-Iva and Thio-Dam exceeded by far the effect of the clinically relevant kinase inhibitor sorafenib (10 µM) (Figure 4b,d).

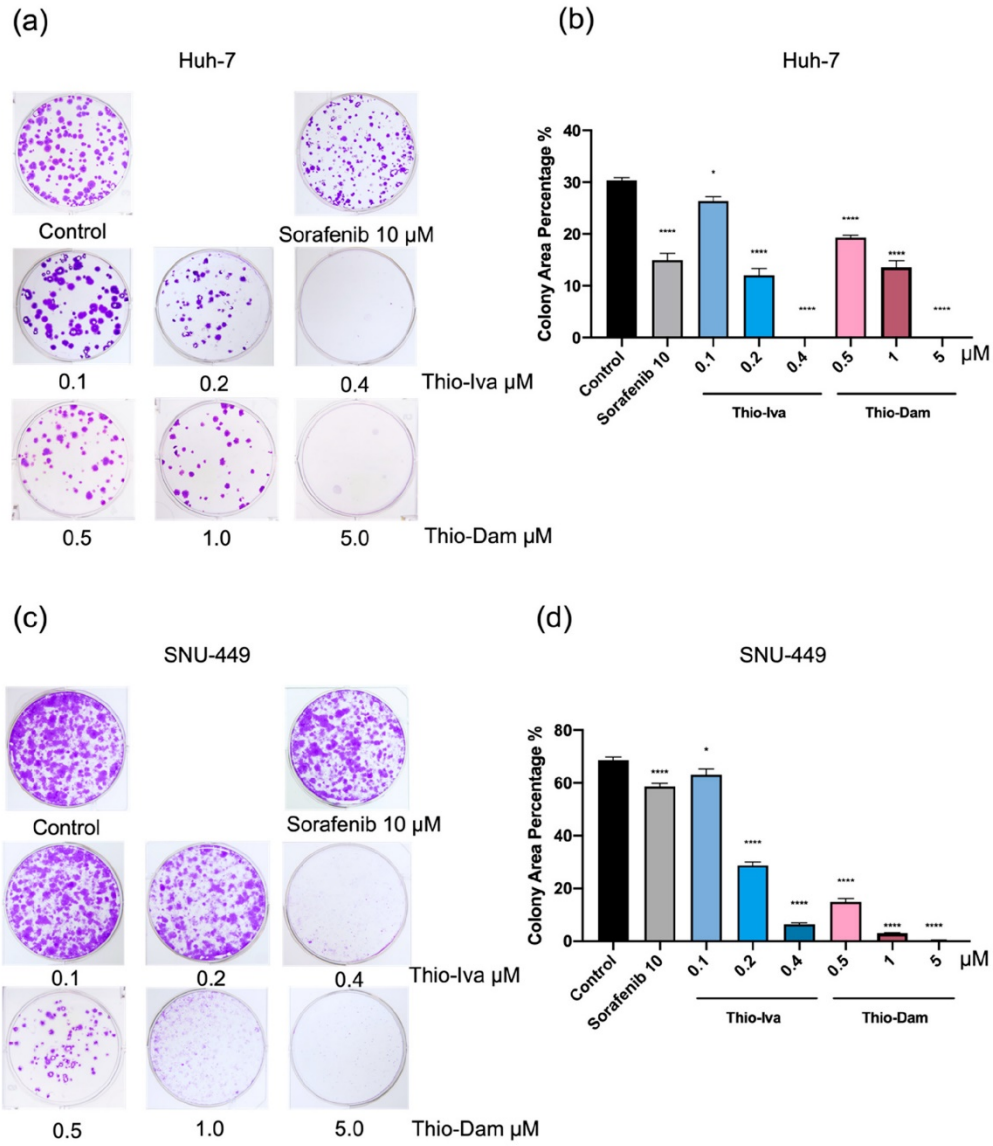

Figure 4. Clonogenic growth. Treatment of Huh-7 (**a**,**b**) and SNU-449 cells (**c**,**d**) with Thio-Iva, Thio-Dam, and sorafenib. The percentage of area occupied by the colonies was quantified using ImageJ software 14 days after plating. * $p < 0.05$ and **** $p < 0.0001$ by ordinary one-way ANOVA compared to control (untreated). All results were expressed as means ± SEM of ≥3 independent experiments.

3.1.4. Unspecific Cytotoxicity

Unspecific cytotoxicity was evaluated by measuring LDH release into the supernatant of the Huh-7 (Figure 5a) and SNU-449 (Figure 5b) cell cultures after incubation for 6 and 24 h with Thio-Iva and Thio-Dam (1 and 10 µM), respectively. An increase of LDH levels in the supernatant indicates the nonspecific damage of cell membranes, which are not permeable to LDH in their undamaged state. However, even upon treatment with a high concentration of 10 µM, neither Thio-Iva nor Thio-Dam induced statistically significant increases in cytotoxicity after 6 h or 24 h, indicating that both compounds do not affect cell

membrane integrity. Thus, an induction of immediate cytotoxicity is unlikely to account for the observed antiproliferative effects of the novel inhibitors.

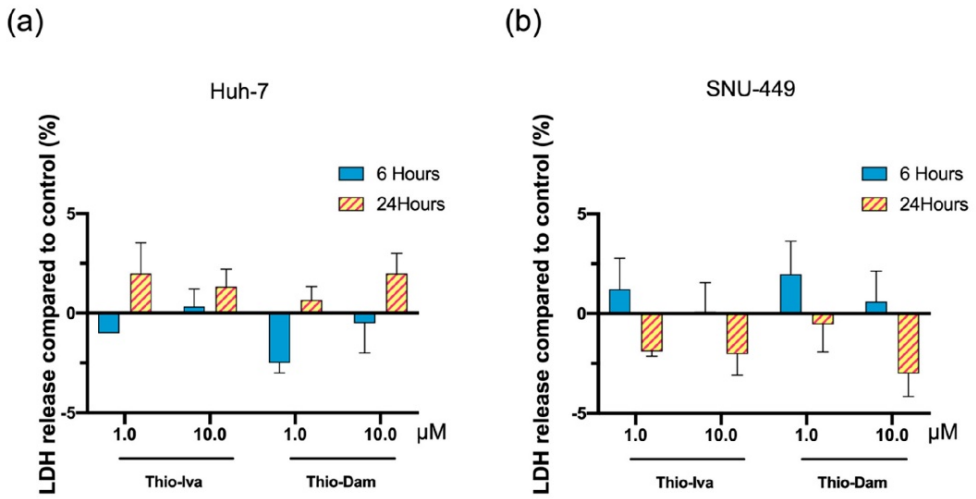

Figure 5. Cytotoxic effects of Thio-Iva and Thio-Dam. Release of lactate dehydrogenase (LDH) after incubation of Huh-7 (**a**) and SNU-449 (**b**) cells with 1 and 10 µM of Thio-Iva and Thio-Dam for 6 and 24 h, respectively. LDH release was not significantly altered when compared to untreated controls (set to 0%), indicating that unspecific toxicity did not contribute to the observed effects. Means ± SD of $n = 3$ independent experiments.

3.1.5. Apoptosis Induction and Regulation in HCC Cells

Apoptosis is the most prominent form of programmed cell death, which is mediated by the activation of effector caspases-3, -6, and -7. As procaspases, these proteases are usually inactive in non-malignant cells, which, however, can undergo autolytic activation upon stimulation to form active caspases. Among these caspases, caspase-3 is responsible for most proteolytic processes during apoptosis. Therefore, the detection of activated caspase-3 is a common marker for apoptosis [25].

Treatment with Thio-Iva and Thio-Dam led to a significant and dose-dependent increase in caspase-3 activity in Huh-7 and SNU-449 cells, which was even stronger than those of sorafenib (10 µM). Thio-Iva and Thio-Dam showed significant dose- and time-dependent increases in caspase-3 activity. At 10 µM, Thio-Iva led to an approximately 3-fold increase when compared with untreated cells, and a 5.5-fold increase after 48 h. For SNU-449, a 3-fold increase was also seen after 24 h, and even a 5.5-fold increase after 48 h. Analogously, Thio-Dam (10 µM) showed a 3.5-fold increase in Huh-7 after 24 h, and a 5-fold increase after 48 h, but only a 2-fold increase was observed for SNU-449 after 48 h (Figure 6a,b).

However, both of the thiophene derivatives induced a more pronounced caspase-3 activation in Huh-7 and SNU-449 cells than sorafenib (10 µM). Western blot analyses revealed that Thio-Iva induced apoptosis so as to promote poly-(ADP-ribose)-polymerase (PARP) cleavage in treated HCC cells (Figure 6c), while the effect of Thio-Dam was less pronounced in SNU-449 cells or was even absent in Huh-7 cells.

Increased formation of reactive oxygen species (ROS) is a cell damage mechanism that plays an important role in cancer development and is also known as a trigger of mitochondria-driven apoptosis. The ROS-specific dye CellROX orange was applied to detect Thio-Iva and Thio-Dam-induced ROS formation in the cytoplasm of Huh-7 cells. After incubation for 24 h, a dose-dependent induction of ROS formation was observed in the cytoplasm of treated cells (Figure 6d).

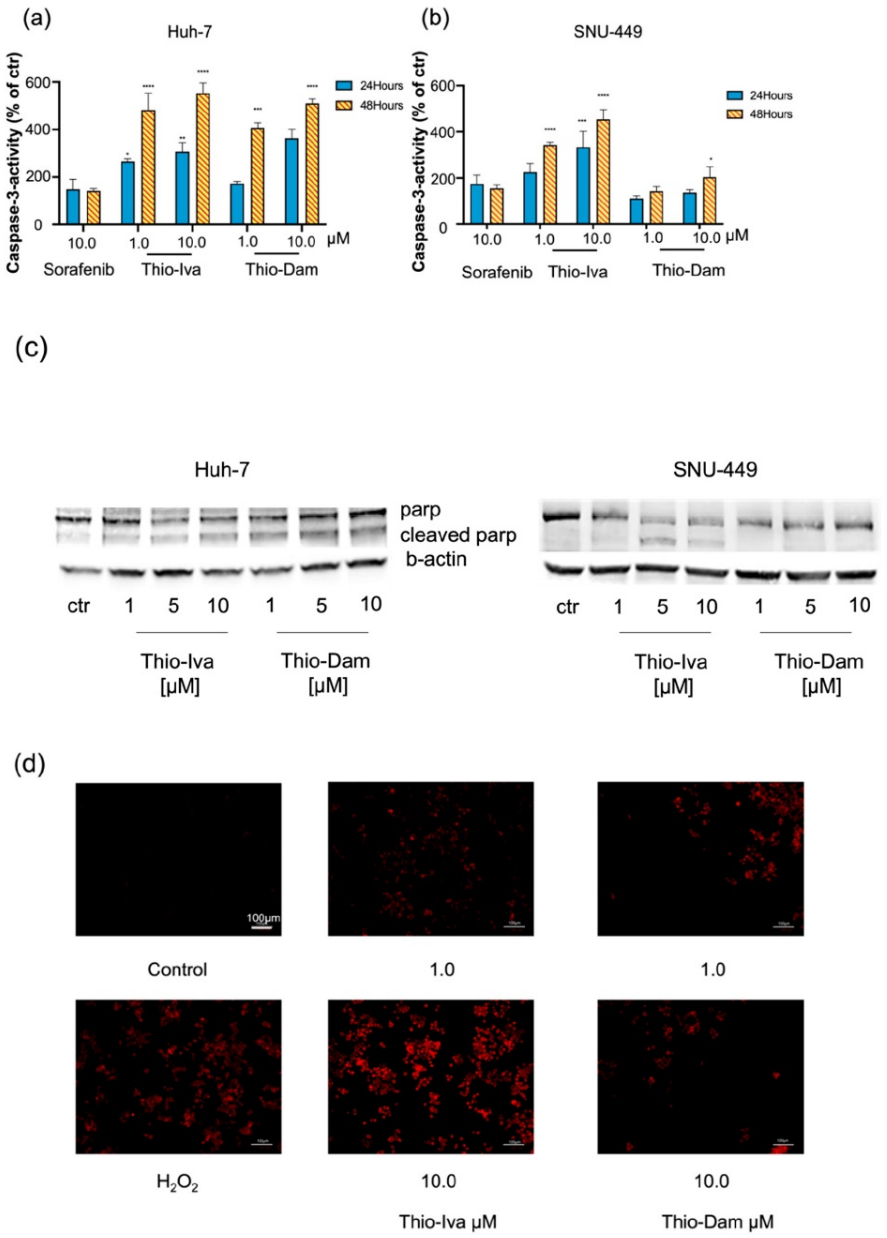

Figure 6. Induction of Apoptosis. (**a**) Dose- and time-dependent caspase-3 induction in Huh-7 cells after treatment with 1 and 10 µM of Thio-Iva and Thio-Dam and 10 µM sorafenib for 24 h and 48 h. (**b**) Dose- and time-dependent caspase-3 induction in SNU-449 cells after treatment with 1 and 10 µM of Thio-Iva and Thio-Dam and 10 µM sorafenib for 24 h and 48 h. Results are given as means ± SEM of $n = 3$ independent experiments. * $p < 0.05$, ** $p < 0.01$, *** $p < 0.001$, and **** $p < 0.0001$ by ordinary one-way ANOVA compared to untreated controls. (**c**) Representative Western blot results out of $n = 3$ independent experiments, showing PARP and cleaved PARP expression change by treatment, induced in Huh-7 and SNU-449 cells after 48 h. β-actin was used as loading control. (**d**) Detection of ROS induction by Thio-Iva and Thio-Dam in HCC cells after 24 h. H_2O_2 served as a positive control. Scale bar, 100 µm.

3.1.6. Cell-Cycle Regulation

The impact of Thio-Iva and Thio-Dam on the cell cycle of Huh-7 and SNU449 cells was determined by flow cytometry. Cells that were treated with 1, 5, and 10 µM of Thio-Iva and Thio-Dam for 48 h showed a dose-dependent and pronounced arrest in the G2/M phase of the cell cycle and a concomitant decrease of cells in the G0/1- and S-phases (Figure 7a–d). By contrast, sorafenib (10 µM) failed to induce a pronounced cell cycle arrest in Huh-7 or SNU-449 cells.

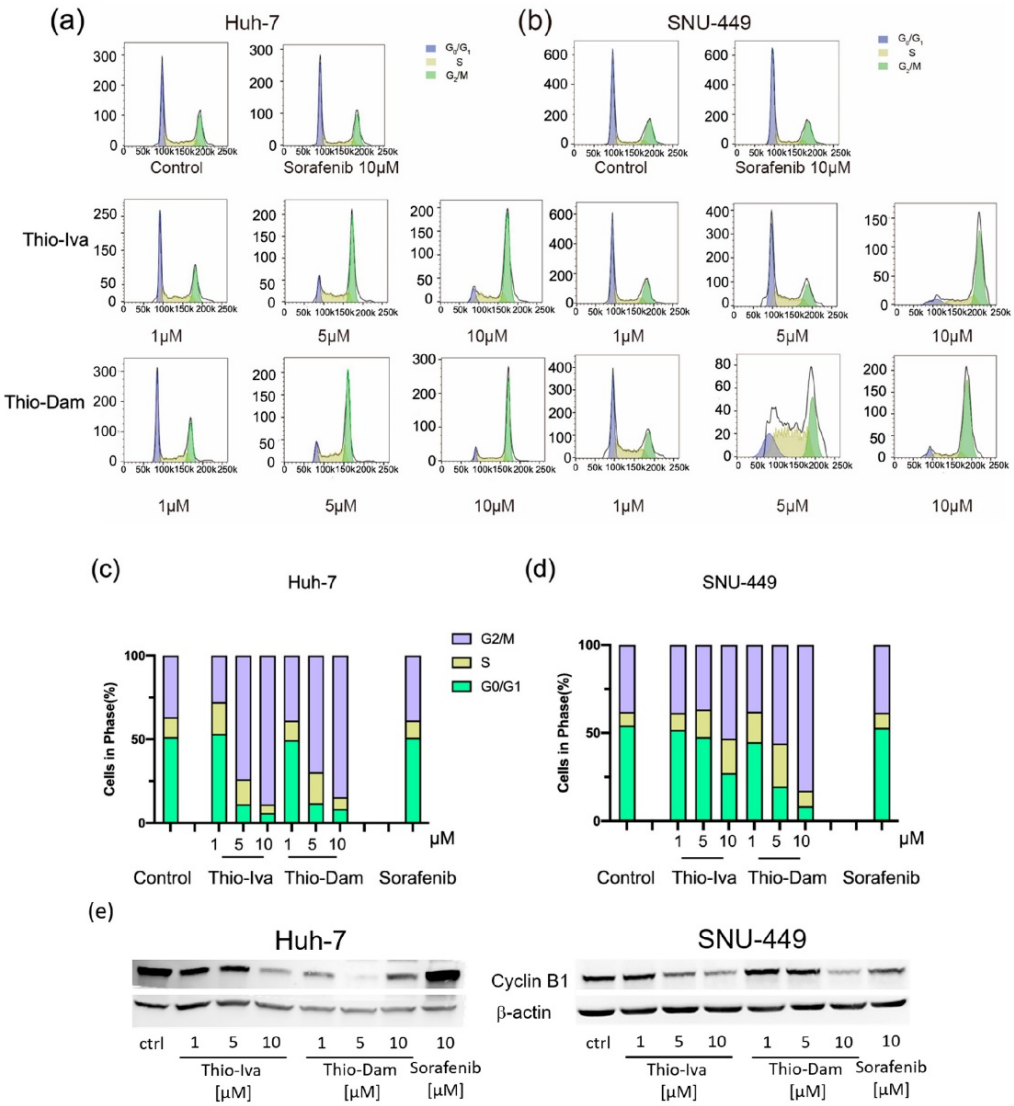

Figure 7. Flow cytometry revealed that Thio-Iva and Thio-Dam induced a pronounced G2/M arrest after 48 h in Huh-7 (**a**) and SNU-449 (**b**) cells. Quantification of the rate of the entire cell cycle; histogram shows average results for Huh-7 (**c**) and SNU-449 (**d**). All results are expressed as means ± SEM of $n = 3$ independent experiments. (**e**) Representative Western blots of $n = 3$ independent experiments showing cyclin B1 expression change in Huh-7 and SNU-449 cells upon treatment for 48 h. ß-actin was used as loading control.

Cyclin B1, a key component in the control of cell cycle progression from the G2 to the M phase, has been implicated in the tumorigenesis and the development of malignancy. Cells suppress and degrade the cell cycle promoter, cyclin B1, in order to escape mitosis [28]. The expression of cyclin B1 was determined to further decipher the molecular mechanism of the G2/M phase blockade by Thio-Iva and Thio-Dam. After 48 h of incubation, both Thio-Iva and Thio-Dam down-regulated cyclin B1 in a dose-dependent manner (Figure 7e), thereby fitting to the flow cytometry findings on a G2/M arrest by the thiophene derivatives in the Huh-7 and SNU-449 cells. The lack of sorafenib to suppress cyclin B1 expression (Figure 7e) corroborates the observation that sorafenib did not induce an appreciable G2/M arrest in either HCC cell line (Figure 7c,d).

3.1.7. Inhibition of Cell Migration

It is mandatory to block the migration and spreading of tumor cells in order to prevent the formation of metastases. Thus, new compounds which inhibit tumor cell migration are of particular interest for the development of new anticancer agents. Wound healing (scratch) assays were performed to investigate the motility of HCC cells treated with Thio-Iva and Thio-Dam (Figure 8). In order to ensure that the scratched gap is filled by migration and not by proliferation, cells were cultured in FBS-free medium for 24 h. The migration rate of untreated Huh-7 control cells was ca. 52.3% after 24 h, while Huh-7 cells treated with Thio-Iva (1, 5, and 10 μM) acted in a dose-dependent way and showed reduced Huh-7 cell migration rates of 33.0%, 19.0%, and 10.0%, respectively. Thio-Dam (1, 5, and 10 μM) showed migration rates of 28.0%, 21.3%, and 16.0%, respectively, which are similar to the rates of Thio-Iva (Figure 8a,c). In SNU-449 cells, the migration rate of untreated control cells was 49.3%, and upon Thio-Iva treatment (1, 5, 10 μM) dropped dose-dependently to 18.3%, 4.6%, and 2.3%, respectively. Comparable results were found for Thio-Dam treatment (1, 5, 10 μM), which resulted in a drop in SNU-449 migration rates of 8.7%, 2.0%, and 1.7%, respectively (Figure 8b,d).

3.1.8. Antiangiogenic Effects of Thio-Iva and Thio-Dam In Vitro and In Vivo

The effects of Thio-Iva and Thio-Dam on angiogenesis were investigated both in vitro and in vivo. Initially, in vitro tube formation assays with endothelial EA.hy926 cells were performed (Figure 9a). Treatment with Thio-Iva led to a strong inhibition of tube formation, with 51% at 0.2 μM and even up to 92% at 1 μM. The effect of Thio-Dam was less pronounced. However, at a dose of 1 μM, Thio-Dam induced an almost 70% inhibition of tube formation (Figure 9b).

In addition, chicken CAM assays were employed to determine the in vivo anti-angiogenic effects of Thio-Iva and Thio-Dam. Both compounds showed considerable reductions of angiogenesis in a dose-dependent way, which were stronger than those of sorafenib, an established anti-angiogenic drug for the treatment of HCC. The vessels displayed morphological irregularities in response to the treatment with Thio-Iva and Thio-Dam, which were not observed in the untreated controls (Figure 9c,d).

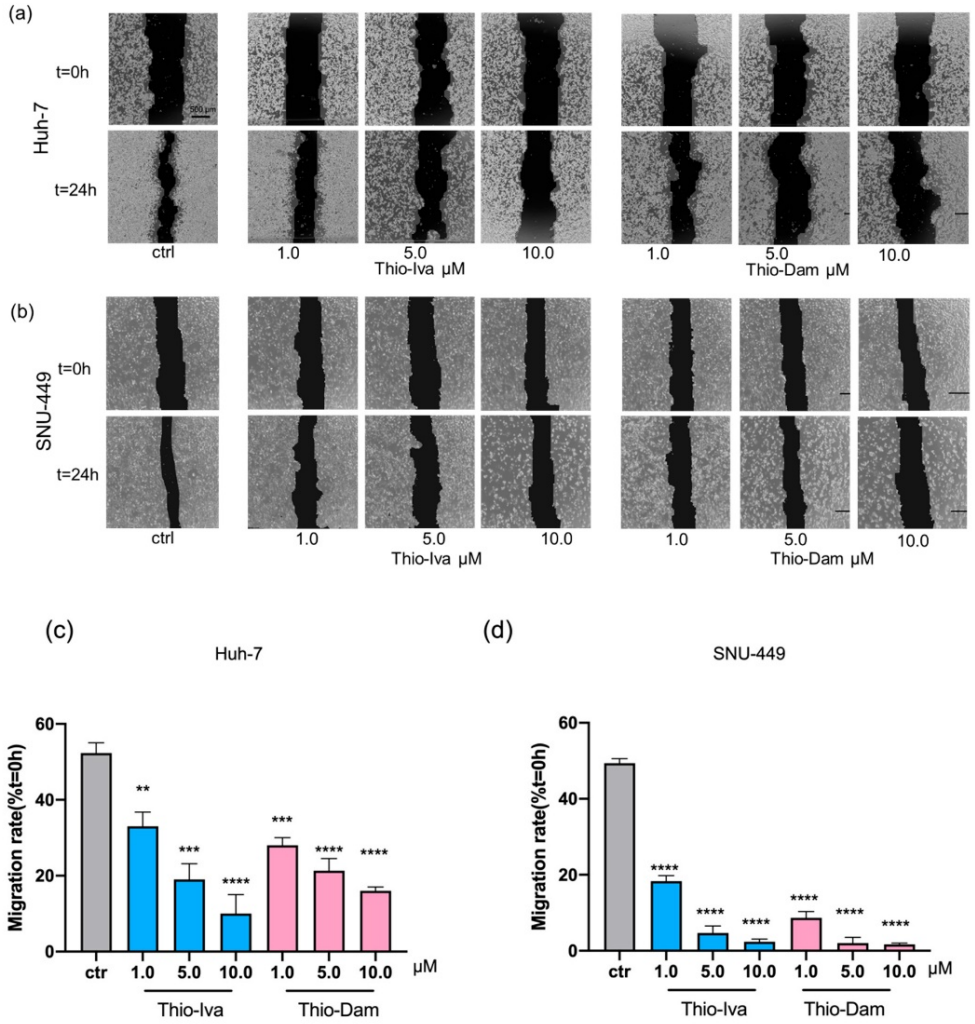

Figure 8. Antimigratory effects of Thio-Iva and Thio-Dam in Huh-7 and SNU-449. (**a**) Representative images of antimigratory effects of Thio-Iva and Thio-Dam (1–10 µM) in Huh-7 cells after 24 h. (**b**) Representative images of antimigratory effects of Thio-Iva and Thio-Dam in SNU-449 cells after 24 h. (**c**,**d**) Quantification of the migration rate (in %) of SNU-449 cells after incubation with Thio-Iva and Thio-Dam. ** $p < 0.01$, *** $p < 0.001$, and **** $p < 0.0001$ by ordinary one-way ANOVA compared to untreated controls. Results are given as means ± SEM of = 3 independent experiments. Scale bar, 500 µm.

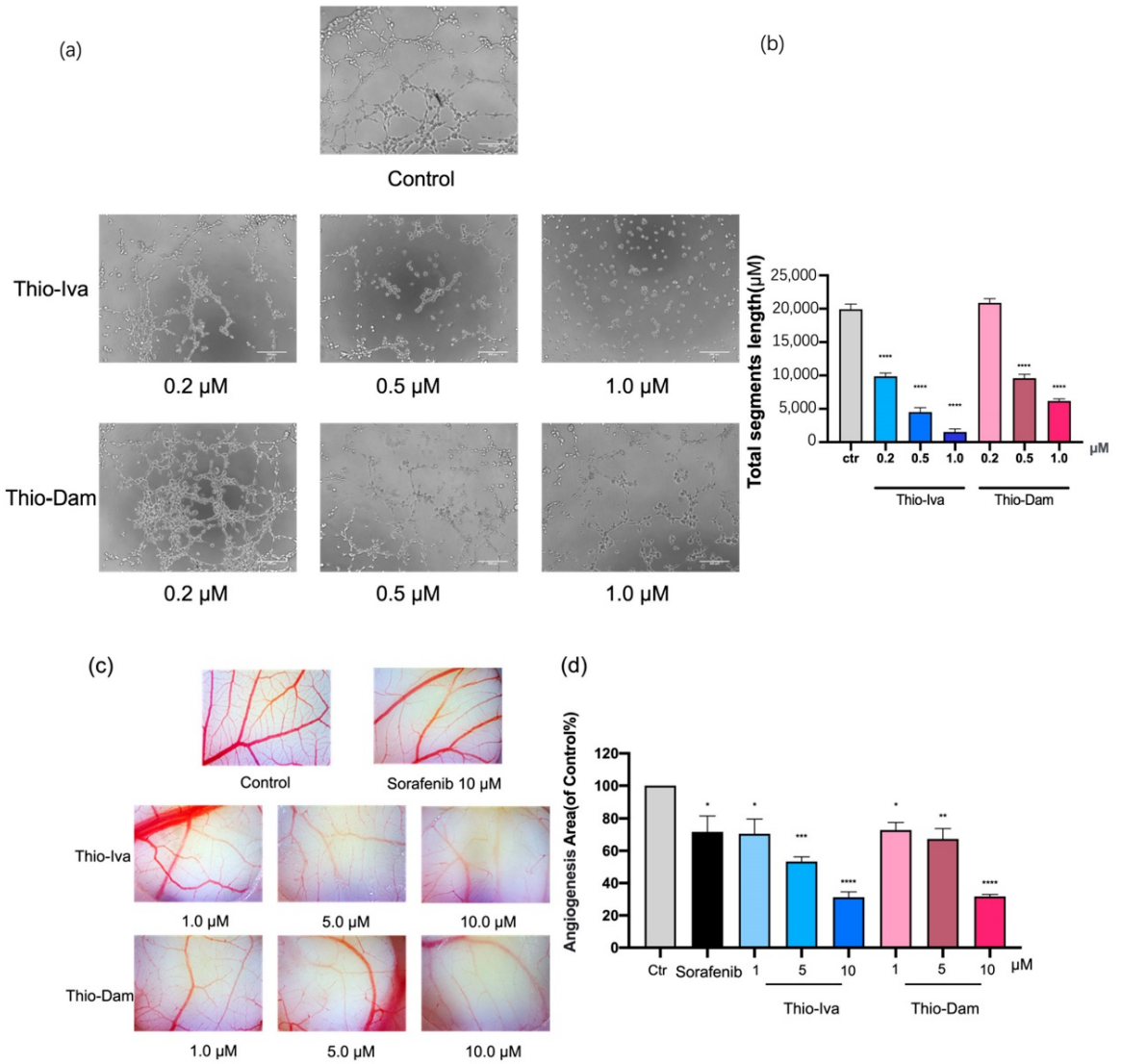

Figure 9. In vitro and in vivo effects of Thio-Iva and Thio-Dam on angiogenesis. (**a**) Representative images of tube formation assay with EA.hy926 cells. Thio-Iva and Thio-Dam (0.2–1 µM) were applied for 6 h. (**b**) Tube formation of EA.hy926 cells was quantified and depicted as changes in total segment length using ImageJ software. (**c**) CAM assay showing inhibition of angiogenesis in vivo: Representative examples of CAM were taken from a typical experiment. Untreated control is the area outside the silica ring. Inside the silicone ring, the surface was treated with different concentrations of Thio-Iva and Thio-Dam for 48 h. (**d**) Image-Pro Plus software was used in analysis for blood vessel area quantification (compared to control in %). * $p < 0.05$, ** $p < 0.01$, *** $p < 0.001$, and **** $p < 0.0001$ by ordinary one-way ANOVA compared to control (untreated area). Results are given as means ± SEM of = 3 independent experiments.

3.1.9. Antineoplastic Effects of Thio-Iva and Thio-Dam In Vivo

CAM assays were performed to demonstrate the effects of Thio-Iva and Thio-Dam on HCC tumor growth in vivo. Micro tumors of Huh-7 cells were grown on the CAM and were treated with Thio-Iva (1–10 µM) and Thio-Dam (1–10 µM) for 72 h. A dose-dependent and highly significant reduction of tumor growth was observed, and the tumor weight decreased by up to 62% (Thio-Iva) and 71% (Thio-Dam), respectively, as compared to PBS-treated controls (Figure 10a,b). Interestingly, sorafenib did not induce a significant reduction of Huh7 microtumor growth in these experiments. It is noteworthy that no increased embryonic lethality rate or signs of developmental retardation was observed in the treated eggs, indicating the good tolerability of the novel compounds—a finding that corroborates the absence of unspecific cytotoxic effects of Thio-Iva and Thio-Dam in Huh-7 and SNU-449 cells in the respective LDH-release assays (Figure 5).

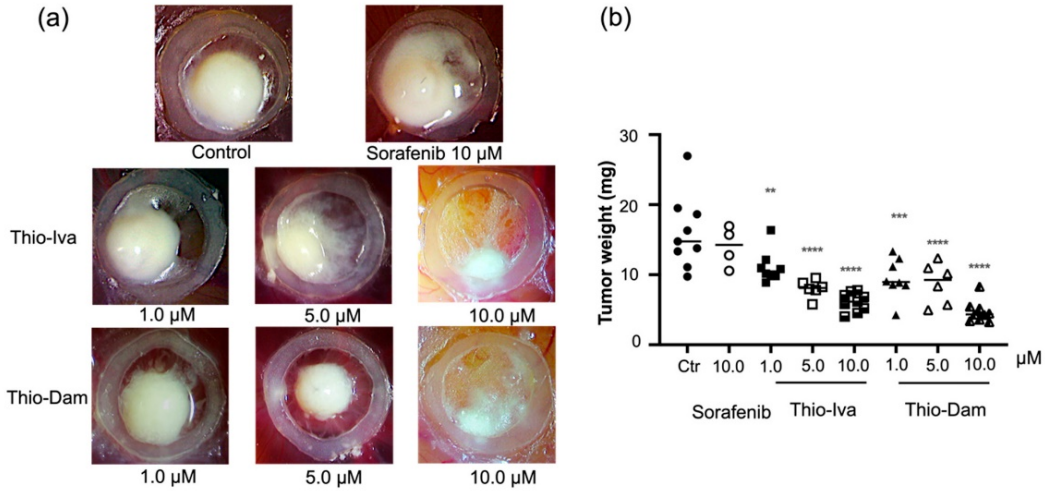

Figure 10. In vivo antineoplastic effects of Thio-Iva and Thio-Dam on Huh-7-derived HCC micro tumors. (**a**) Representative images of Thio-Iva and Thio-Dam-treated microtumors grown on the CAM of fertilized chicken eggs after 72 h. Sorafenib was additionally applied as a clinically relevant HCC therapeutic. PBS-treated microtumors served as controls. (**b**) Tumor weight analysis. ** $p < 0.01$, *** $p < 0.001$, and **** $p < 0.0001$ by ordinary one-way ANOVA compared to controls. Results are shown as means ± SEM of = 3 independent experiments.

4. Discussion

Hepatocellular carcinoma is the fourth leading cause of cancer death in the world, which accounts for more than 80% of global primary liver cancers [29]. In recent years, significant progress has been made in terms of surgical treatment, interventional therapy, and radiotherapy for patients suffering from early HCC [3,30]. However, medical treatment methods for patients with advanced HCC showed only marginal improvements in efficacy [31]. Therefore, there is an urgent need for new drugs for the treatment of advanced HCC. Recently, we introduced a series of 2-(thien-2-yl)-acrylonitriles with different aryl substituents (such as hydroxyl and alkoxy, dialkylamine, and halogen) as protein kinase inhibitory compounds with antineoplastic potency [21].

In the present study, the anti-tumor effects of Thio-Iva and Thio-Dam, the two most effective compounds of the series, were further elaborated in terms of their anticancer properties in two HCC cell models. Their underlying modes of action were deciphered as well as their antineoplastic and anti-angiogenic effects in vivo.

Aggressive tumors are characterized by a sustained proliferation of tumor cells. We showed that the compounds Thio-Iva and Thio-Dam exert strong antiproliferative effects

on HCC cells in a dose- and time-dependent manner, which even exceeded those of the clinically approved multi-kinase inhibitor sorafenib. In addition, real-time proliferation monitoring revealed that Thio-Iva and Thio-Dam exerted their growth inhibitory effects after only 12 and 24 h, respectively. In addition, colony formation assays showed the long-term anti-proliferative effects of the novel thiophene derivatives, while the anticancer effects of Thio-Iva and Thio-Dam were not based on the induction of unspecific cytotoxicity but involved the induction of apoptosis and cell cycle arrest as specific modes of action.

As the evasion of apoptosis by cancer cells is one of the leading causes of uncontrolled tumor cell growth, the acquisition of anti-apoptotic features during carcinogenesis is regarded as one of the hallmarks of cancer [32]. The cysteine protease caspase-3 is the most important executioner caspase of cellular apoptosis [33], and thus its induction by Thio-Iva and Thio-Dam was determined as an unequivocal sign of apoptosis induction in Huh-7 and SNU-449 cells. Treatment with Thio-Iva and Thio-Dam in a time- and dose-dependent manner induced caspase-3 activity, which even exceeded by far those of sorafenib. The increase of ROS levels can promote the dissipation of mitochondrial membrane potential, can cause organ dysfunction, and can trigger mitochondria-driven apoptosis. Moreover, excessive ROS levels are also related to DNA damage [34]. Thio-Iva and Thio-Dam were shown to induce pronounced increases in cytoplasmic ROS levels. Mitochondria are the main source of ROS in cells and the most severely affected organelles of cellular stress [35]. In order to link the Thio-Iva and Thio-Dam-induced rise in cytoplasmic ROS to the mitochondria-driven apoptosis of HCC cells, we demonstrated in this study that the acute burst of ROS in mitochondria specifically causes cell apoptosis and subsequently activates caspase-3. Western blotting showed that PARP, the substrate of caspase-3, was reduced and cleaved into an N-terminal 89 kDa fragment in the Huh-7 cell line incubated with Thio-Iva. Albeit less pronounced, Thio-Dam treatment also decreased PARP expression, at least in SNU-449 cells.

In terms of DNA damage, blocking cell-cycle checkpoints can lead to genome instability and subsequent cell death. G2 abolition prevents cancer cells from repairing DNA damage, forcing them to enter the M phase and the so-called "mitotic catastrophe" as well as apoptosis [36,37]. The G2 checkpoint has become an attractive therapeutic target for anticancer therapy. Flow cytometry analyses revealed a dose-dependent G2/M phase arrest in Huh-7 and SNU-449 cells treated with Thio-Iva and Thio-Dam. These compounds meet the criteria of ideal G2 checkpoint inhibitors, which selectively target molecules that do not participate in the G1 checkpoint or S phase checkpoints [38]. The precise regulation of cyclin B1 is essential for the onset of mitosis and for checkpoint control. It was also shown to regulate cell cycle transition from the G2 to the M phase [39,40]. Thio-Iva and Thio-Dam significantly suppressed cyclin B1 in both cell lines after 48 h, while treatment with sorafenib only had slight effects on cyclin B1 expression, which is in line with our findings from the flow cytometry experiments. More and more evidence suggest that cyclin B1 is highly expressed in several tumors, and its effects were correlated with tumor proliferation, invasion, and apoptosis [40,41]. The distinct suppression of cyclin B1 by Thio-Iva and Thio-Dam can explain the pronounced pro-apoptotic activities of these compounds.

As a malignant, hyper-vascularized solid tumor, HCC can be treated by inhibiting angiogenesis. Tumor angiogenesis is regarded as another hallmark of cancer [32] and may thus be an important target in HCC treatment. Sorafenib inhibits multiple receptor tyrosine kinases such as the VEGFR and PDGFR signaling pathways and has been the first-line drug in the treatment of advanced HCC for a long time [2]. However, a considerable number of HCC patients had to stop sorafenib treatment due to unbearable side effects or drug resistance. Therefore, some other multi-kinase inhibitors such as brivanib, sunitinib, and linifanib were studied, but these failed in phase III trials [11,42,43]. VEGFR-2 is a transmembrane receptor tyrosine kinase that functions in both physiological and pathological angiogenesis. The activation of VEGFR-2 promotes endothelial cell invasion, migration, proliferation, and angiogenesis [44,45]. However, the VEGFR-2 inhibitor ramucirumab also failed to reach the end point in a recent phase III trial [10]. Thio-Iva and Thio-Dam

were recently described as novel multi-kinase inhibitors with preferential VEGF Receptor inhibition [21]. Endothelial cells are involved in angiogenesis and proliferate to provide the cells required to form new blood vessels. After proliferation, endothelial cells reorganize into a three-dimensional tubular structure [46]. Our in vitro experiments demonstrated that Thio-Iva and Thio-Dam affect EA.hy926 cell tube formation even at low concentrations. In particular, cells treated with Thio-Iva displayed no tubular structure at all. In addition, CAM assays showed that Thio-Iva and Thio-Dam also reduced angiogenesis in vivo and to a higher degree than sorafenib. Vessels in treated CAMs displayed visible morphological irregularities (Figure 7b).

As a prerequisite for invasion and metastasis, the migration of tumor cells is regarded as another hallmark of cancer [32]. HCC cells treated with Thio-Iva and Thio-Dam showed significantly decreased cell migration, indicating that both compounds exert anti-metastatic properties.

The CAM assay is an established model for testing anti-tumor compounds in vivo and can be used as a template for growing micro tumors from human cancer cell lines [47]. We showed that Thio-Iva and Thio-Dam reduce the growth of HCC tumors grown on CAMs, thus confirming their considerable antineoplastic effects in vivo. Both compounds were well-tolerated and did not exhibit embryo toxicity or developmental delay. The effects of the novel thiophene-based compounds were also notably more effective than the treatment with the clinically established multi-kinase inhibitor sorafenib.

5. Conclusions

In conclusion, we demonstrated the pronounced antiproliferative, apoptosis-inducing, antimigratory, and cell cycle-arresting properties of the two novel 2-(thien-2-yl)-acrylonitrile kinase inhibitors in HCC cells. In addition, Thio-Iva and Thio-Dam showed significant antitumor and antiangiogenic effects as well as excellent in vivo tolerance. The novel compounds were shown to effectively attack HCC cells in cellular processes and features that are acquired during carcinogenesis and which are referred to as hallmarks of cancer. Our results show that Thio-Iva and Thio-Dam may provide new and valuable options for the treatment of hepatocellular carcinoma in the future. Hence, future investigations of these promising kinase inhibitors are warranted.

Author Contributions: Conceptualization, M.H. and B.N.; methodology, A.M. and B.N.; software, A.M. and N.G.; validation, M.H., B.B., B.N. and A.M.; formal analysis, A.M.; investigation, A.M. and N.G.; resources, M.H. and B.N.; data curation, A.M. and B.N.; writing—original draft preparation, A.M. and B.B.; writing—review and editing, B.N., M.H. and B.B.; visualization, A.M., N.G. and B.N.; supervision, M.H. and B.N.; project administration, M.H. All authors have read and agreed to the published version of the manuscript.

Funding: This research received no external funding.

Institutional Review Board Statement: Not applicable.

Informed Consent Statement: Informed consent was obtained from all subjects involved in the study.

Data Availability Statement: Not applicable.

Acknowledgments: We thank Lili Liang from Charité Universitätsmedizin Berlin, Klinik für Gynäkologie, Forschung (Labor), Campus Virchow Klinikum for her excellent support in the FACS experiments.

Conflicts of Interest: The authors declare no conflict of interest.

References

1. Villanueva, A. Hepatocellular carcinoma. *N. Engl. J. Med.* **2019**, *380*, 1450–1462. [CrossRef] [PubMed]
2. Llovet, J.M.; Kelley, R.K.; Villanueva, A.; Singal, A.G.; Pikarsky, E.; Roayaie, S.; Lencioni, R.; Koike, K.; Zucman-Rossi, J.; Finn, R.S. Hepatocellular carcinoma. *Nat. Rev. Dis. Primers* **2021**, *7*, 6. [CrossRef] [PubMed]
3. Llovet, J.M.; Zucman-Rossi, J.; Pikarsky, E.; Sangro, B.; Schwartz, M.; Sherman, M.; Gores, G. Hepatocellular carcinoma. *Nat. Rev. Dis. Primers* **2016**, *2*, 1–52. [CrossRef] [PubMed]

4. Tang, W.; Chen, Z.; Zhang, W.; Cheng, Y.; Zhang, B.; Wu, F.; Wang, Q.; Wang, S.; Rong, D.; Reiter, F.P.; et al. The mechanisms of sorafenib resistance in hepatocellular carcinoma: Theoretical basis and therapeutic aspects. *Signal Transduct. Target. Ther.* **2020**, *5*, 87. [CrossRef] [PubMed]
5. Jiao, Q.; Bi, L.; Ren, Y.; Song, S.; Wang, Q.; Wang, Y.S. Advances in studies of tyrosine kinase inhibitors and their acquired resistance. *Mol. Cancer* **2018**, *17*, 36. [CrossRef] [PubMed]
6. Liu, L.; Cao, Y.; Chen, C.; Zhang, X.; McNabola, A.; Wilkie, D.; Wilhelm, S.; Lynch, M.; Carter, C. Sorafenib blocks the RAF/MEK/ERK pathway, inhibits tumor angiogenesis, and induces tumor cell apoptosis in hepatocellular carcinoma model PLC/PRF/5. *Cancer Res.* **2006**, *66*, 11851–11858. [CrossRef]
7. Josep, M.; Llovet, S.R.; Mazzaferro, V.; Hilgard, P.; Gane, E.; Blanc, J.F.; de Oliveira, A.C.; Santoro, A.; Raoul, J.L.; Forner, A.; et al. Sorafenib in advanced hepatocellular carcinoma. *N. Engl. J. Med.* **2008**, *359*, 12.
8. Gauthier, A.; Ho, M. Role of sorafenib in the treatment of advanced hepatocellular carcinoma: An update. *Hepatol. Res.* **2013**, *43*, 147–154. [CrossRef]
9. Cheng, A.-L.; Kang, Y.-K.; Chen, Z.; Tsao, C.-J.; Qin, S.; Kim, J.S.; Luo, R.; Feng, J.; Ye, S.; Yang, T.S.; et al. Efficacy and safety of sorafenib in patients in the Asia-Pacific region with advanced hepatocellular carcinoma: A phase III randomised, double-blind, placebo-controlled trial. *Lancet Oncol.* **2009**, *10*, 25–34. [CrossRef]
10. Zhu, A.X.; Kang, Y.-K.; Yen, C.-J.; Finn, R.S.; Galle, P.R.; Llovet, J.M.; Assenat, E.; Brandi, G.; Pracht, M.; Lim, H.Y.; et al. Ramucirumab after sorafenib in patients with advanced hepatocellular carcinoma and increased α-fetoprotein concentrations (REACH-2): A randomised, double-blind, placebo-controlled, phase 3 trial. *Lancet Oncol.* **2019**, *20*, 282–296. [CrossRef]
11. Cainap, C.; Qin, S.; Huang, W.T.; Chung, I.J.; Pan, H.; Cheng, Y.; Kudo, M.; Kang, Y.K.; Chen, P.J.; Toh, H.C.; et al. Linifanib versus Sorafenib in patients with advanced hepatocellular carcinoma: Results of a randomized phase III trial. *J. Clin. Oncol.* **2015**, *33*, 172–179. [CrossRef] [PubMed]
12. Kudo, M.; Finn, R.S.; Qin, S.; Han, K.-H.; Ikeda, K.; Piscaglia, F.; Baron, A.; Park, J.W.; Han, G.; Jassem, J.; et al. Lenvatinib versus sorafenib in first-line treatment of patients with unresectable hepatocellular carcinoma: A randomised phase 3 non-inferiority trial. *Lancet* **2018**, *391*, 1163–1173. [CrossRef]
13. El-Khoueiry, A.B.; Sangro, B.; Yau, T.; Crocenzi, T.S.; Kudo, M.; Hsu, C.; Kim, T.Y.; Choo, S.P.; Trojan, J.; Welling, T.H., 3rd; et al. Nivolumab in patients with advanced hepatocellular carcinoma (CheckMate 040): An open-label, non-comparative, phase 1/2 dose escalation and expansion trial. *Lancet* **2017**, *389*, 2492–2502. [CrossRef]
14. Morse, M.A.; Sun, W.; Kim, R.; He, A.R.; Abada, P.B.; Mynderse, M.; Finn, R.S. The role of angiogenesis in hepatocellular carcinoma. *Clin. Cancer Res.* **2019**, *25*, 912–920. [CrossRef]
15. Avraamides, C.J.; Garmy-Susini, B.; Varner, J.A. Integrins in angiogenesis and lymphangiogenesis. *Nat. Rev. Cancer* **2008**, *8*, 604–617. [CrossRef]
16. Chung, A.S.; Ferrara, N. Developmental and pathological angiogenesis. *Annu. Rev. Cell Dev. Biol.* **2011**, *27*, 563–584. [CrossRef]
17. Zirlik, K.; Duyster, J. Anti-angiogenics: Current situation and future perspectives. *Oncol. Res. Treat.* **2018**, *41*, 166–171. [CrossRef]
18. Ribatti, D.; Pezzella, F. Overview on the different patterns of tumor vascularization. *Cells* **2021**, *10*, 639. [CrossRef]
19. Karunakaran, J.; Dhatchana Moorthy, N.; Chowdhury, S.R.; Iqbal, S.; Majumder, H.K.; Gunasekaran, K.; Vellaichamy, E.; Mohanakrishnan, A.K. Divergent synthesis and evaluation of the in vitro cytotoxicity profiles of 3,4-ethylenedioxythiophenyl-2-propen-1-one analogues. *ChemMedChem* **2019**, *14*, 1418–1430. [CrossRef]
20. Quiroga, J.; Cobo, D.; Insuasty, B.; Abonia, R.; Nogueras, M.; Cobo, J.; Vasquez, Y.; Gupta, M.; Derita, M.; Zacchino, S. Synthesis and evaluation of novel E-2-(2-thienyl)- and Z-2-(3-thienyl)-3-arylacrylonitriles as antifungal and anticancer agents. *Arch. Pharm. Weinh.* **2007**, *340*, 603–606. [CrossRef]
21. Schaller, E.; Ma, A.; Gosch, L.C.; Klefenz, A.; Schaller, D.; Goehringer, N.; Kaps, L.; Schuppan, D.; Volkamer, A.; Schobert, R.; et al. New 3-aryl-2-(2-thienyl) acrylonitriles with high activity against hepatoma cells. *Int. J. Mol. Sci.* **2021**, *22*, 2243. [CrossRef] [PubMed]
22. Steinemann, G.; Dittmer, A.; Kuzyniak, W.; Hoffmann, B.; Schrader, M.; Schobert, R.; Biersack, B.; Nitzsche, B.; Hoepfner, M. Animacroxam, a novel dual-mode compound targeting histone deacetylases and cytoskeletal integrity of testicular germ cell cancer cells. *Mol. Cancer Ther.* **2017**, *16*, 2364–2374. [CrossRef] [PubMed]
23. Goehringer, N.; Biersack, B.; Peng, Y.; Schobert, R.; Herling, M.; Ma, A.; Nitzsche, B.; Höpfner, M. Anticancer activity and mechanisms of action of new chimeric EGFR/HDAC-inhibitors. *Int. J. Mol. Sci.* **2021**, *22*, 8432. [CrossRef]
24. Bender, O.; Llorent-Martinez, E.J.; Zengin, G.; Mollica, A.; Ceylan, R.; Molina-Garcia, L.; Fernández-de Córdova, M.L.; Atalay, A. Integration of in vitro and in silico perspectives to explain chemical characterization, biological potential and anticancer effects of Hypericum salsugineum: A pharmacologically active source for functional drug formulations. *PLoS ONE* **2018**, *13*, e0197815. [CrossRef] [PubMed]
25. Crowley, L.C.; Waterhouse, N.J. Detecting cleaved caspase-3 in apoptotic cells by flow cytometry. *Cold Spring Harb. Protoc.* **2016**, *2016*, pdb-prot087312. [CrossRef] [PubMed]
26. Goehringer, N.; Peng, Y.; Nitzsche, B.; Biermann, H.; Pradhan, R.; Schobert, R.; Herling, M.; Höpfner, M.; Biersack, B. Improved anticancer activities of a new pentafluorothio-substituted vorinostat-type histone deacetylase inhibitor. *Pharmaceuticals* **2021**, *14*, 1319. [CrossRef] [PubMed]
27. Ogbodu, R.O.; Nitzsche, B.; Ma, A.; Atilla, D.; Gurek, A.G.; Hopfner, M. Photodynamic therapy of hepatocellular carcinoma using tetra-triethyleneoxysulfonyl zinc phthalocyanine as photosensitizer. *J. Photochem. Photobiol. B* **2020**, *208*, 111915. [CrossRef]

28. Pawlik, T.M.; Keyomarsi, K. Role of cell cycle in mediating sensitivity to radiotherapy. *Int. J. Radiat. Oncol. Biol. Phys.* **2004**, *59*, 928–942. [CrossRef]
29. Yang, J.D.; Hainaut, P.; Gores, G.J.; Amadou, A.; Plymoth, A.; Roberts, L.R. A global view of hepatocellular carcinoma: Trends, risk, prevention and management. *Nat. Rev. Gastroenterol. Hepatol.* **2019**, *16*, 589–604. [CrossRef]
30. Marrero, J.A.; Kulik, L.M.; Sirlin, C.B.; Zhu, A.X.; Finn, R.S.; Abecassis, M.M.; Roberts, L.R.; Heimbach, J.K. Diagnosis, staging, and management of hepatocellular carcinoma: 2018 practice guidance by the American association for the study of liver diseases. *Hepatology* **2018**, *68*, 723–750. [CrossRef]
31. Lim, H.; Ramjeesingh, R.; Liu, D.; Tam, V.C.; Knox, J.J.; Card, P.B.; Meyers, B.M. Optimizing survival and the changing landscape of targeted therapy for intermediate and advanced hepatocellular carcinoma: A systematic review. *J. Natl. Cancer Inst.* **2021**, *113*, 123–136. [CrossRef] [PubMed]
32. Hanahan, D. Hallmarks of cancer: New dimensions. *Cancer Discov.* **2022**, *12*, 31–46. [CrossRef] [PubMed]
33. Huang, Q.; Li, F.; Liu, X.; Li, W.; Shi, W.; Liu, F.F.; O'sullivan, B.; He, Z.; Peng, Y.; Tan, A.C.; et al. Caspase 3-mediated stimulation of tumor cell repopulation during cancer radiotherapy. *Nat. Med.* **2011**, *17*, 860–866. [CrossRef] [PubMed]
34. Srinivas, U.S.; Tan, B.W.Q.; Vellayappan, B.A.; Jeyasekharan, A.D. ROS and the DNA damage response in cancer. *Redox Biol.* **2019**, *25*, 101084. [CrossRef]
35. Izyumov, D.S.; Domnina, L.V.; Nepryakhina, O.K.; Avetisyan, A.V.; Golyshev, S.A.; Ivanova, O.Y.; Korotetskaya, M.V.; Lyamzaev, K.G.; Pletjushkina, O.Y.; Popova, E.N.; et al. Mitochondria as source of reactive oxygen species under oxidative stress. Study with novel mitochondria-targeted antioxidants—The "Skulachev-ion" derivatives. *Biochem. Mosc.* **2010**, *75*, 123–129. [CrossRef]
36. Matheson, C.J.; Backos, D.S.; Reigan, P. Targeting WEE1 kinase in cancer. *Trends Pharmacol. Sci.* **2016**, *37*, 872–881. [CrossRef]
37. Bucher, N.; Britten, C.D. G2 checkpoint abrogation and checkpoint kinase-1 targeting in the treatment of cancer. *Br. J. Cancer* **2008**, *98*, 523–528. [CrossRef]
38. Kawabe, T. G2 checkpoint abrogators as anticancer drugs. *Mol. Cancer Ther.* **2004**, *3*, 7.
39. Gavet, O.; Pines, J. Progressive activation of CyclinB1-Cdk1 coordinates entry to mitosis. *Dev. Cell* **2010**, *18*, 533–543. [CrossRef]
40. Tang, L.; Zhang, Y.; Pan, H.; Luo, Q.; Zhu, X.M.; Dong, M.Y.; Leung, P.C.; Sheng, J.Z.; Huang, H.F. Involvement of cyclin B1 in progesterone-mediated cell growth inhibition, G2/M cell cycle arrest, and apoptosis in human endometrial cell. *Reprod. Biol. Endocrinol.* **2009**, *7*, 144. [CrossRef]
41. Yuan, J.; Yan, R.; Kramer, A.; Eckerdt, F.; Roller, M.; Kaufmann, M.; Strebhardt, K. Cyclin B1 depletion inhibits proliferation and induces apoptosis in human tumor cells. *Oncogene* **2004**, *23*, 5843–5852. [CrossRef] [PubMed]
42. Llovet, J.M.; Decaens, T.; Raoul, J.L.; Boucher, E.; Kudo, M.; Chang, C.; Kang, Y.K.; Assenat, E.; Lim, H.Y.; Boige, V.; et al. Brivanib in patients with advanced hepatocellular carcinoma who were intolerant to sorafenib or for whom sorafenib failed: Results from the randomized phase III BRISK-PS study. *J. Clin. Oncol.* **2013**, *31*, 3509–3516. [CrossRef] [PubMed]
43. Cheng, A.L.; Kang, Y.K.; Lin, D.Y.; Park, J.W.; Kudo, M.; Qin, S.; Chung, H.C.; Song, X.; Xu, J.; Poggi, G.; et al. Sunitinib versus sorafenib in advanced hepatocellular cancer: Results of a randomized phase III trial. *J. Clin. Oncol.* **2013**, *31*, 4067–4075. [CrossRef] [PubMed]
44. Shibuya, M.; Claesson-Welsh, L. Signal transduction by VEGF receptors in regulation of angiogenesis and lymphangiogenesis. *Exp. Cell Res.* **2006**, *312*, 549–560. [CrossRef] [PubMed]
45. Ferrara, N.; Gerber, H.P.; LeCouter, J. The biology of VEGF and its receptors. *Nat. Med.* **2003**, *9*, 669–676. [CrossRef]
46. Cao, J.; Liu, X.; Yang, Y.; Wei, B.; Li, Q.; Mao, G.; He, Y.; Li, Y.; Zheng, L.; Zhang, Q.; et al. Decylubiquinone suppresses breast cancer growth and metastasis by inhibiting angiogenesis via the ROS/p53/BAI1 signaling pathway. *Angiogenesis* **2020**, *23*, 325–338. [CrossRef]
47. Deryugina, E.I.; Quigley, J.P. Chick embryo chorioallantoic membrane model systems to study and visualize human tumor cell metastasis. *Histochem. Cell Biol.* **2008**, *130*, 1119–1130. [CrossRef]

Curriculum Vitae

My CV will not be published in the electronic version of my thesis for data protection reasons.

Publication list

Journal Publications:

1. **Ma A**, Biersack B, Goehringer N, Nitzsche B, Höpfner M. Novel Thienyl-Based Tyrosine Kinase Inhibitors for the Treatment of Hepatocellular Carcinoma. J Pers Med. 2022 May 1;12(5):738. **IF:4.945**

2. Schaller E, **Ma A**, Gosch LC, Klefenz A, Schaller D, Goehringer N, Kaps L, Schuppan D, Volkamer A, Schobert R, Biersack B, Nitzsche B, Höpfner M. New 3-Aryl-2-(2-thienyl) acrylonitriles with High Activity Against Hepatoma Cells. Int J Mol Sci. 2021 Feb 24;22(5):2243. **IF:6.208**

3. Ogbodu RO, Nitzsche B, **Ma A**, Atilla D, Gürek AG, Höpfner M. Photodynamic therapy of hepatocellular carcinoma using tetra-triethyleneoxysulfonyl zinc phthalocyanine as photosensitizer. J Photochem Photobiol B. 2020 Jul; 208:111915. **IF:6.814**

4. Goehringer N, Biersack B, Peng Y, Schobert R, Herling M, **Ma A**, Nitzsche B, Höpfner M. Anticancer Activity and Mechanisms of Action of New Chimeric EGFR/HDAC-Inhibitors. Int J Mol Sci. 2021 Aug 5;22(16):8432. **IF:6.208**

Acknowledgments

Now that I have finished writing this chapter, I would like to take this opportunity to thank all the people who have given me valuable support and help.

First of all, I would like to express my deep gratitude to Prof. Michael Höpfner for giving me the opportunity to study and work in their lab for my MD degree. During the three years of work, you encouraged me and provided great project ideas. In addition, I would like to thank Prof. Bianca Nitzsche for guiding and motivating me to do better science, and you always supported me with constant patience and fruitful discussions.

Furthermore, I would like to thank Bernhard Biersack for collaborating with us and providing research support, Gustav Steinemann, Nils Goehringer, Kehle Lisa for scientific discussions and unlimited support, which really encouraged me to continue my project. Special thanks to Racheal O Ogbodu, you were always very enthusiastic to help me with various difficulties inside and outside the lab and your positive attitude towards life was always a great encouragement to me. I am very grateful to Hoffmann Björn for the great technical support. In addition, I would like to thank all the members of the Michael Höpfner lab for all the happy and sad moments when we worked together.

Besides, I want to thank my friends Dai Dai, Liang Lili, Tao Yongyi for all the laughs we had together.

Finally, I would like to thank my family for your continuous supporting and encouraging me, shaping me to the person that I am.

Thank you all.

Andi Ma